

SEDIMENT DYNAMICS ON THE PALOS VERDES SHELF

**A REPORT SUBMITTED TO
THE LOS ANGELES COUNTY SANITATION DISTRICT**

**BY
SUZANNE REYNOLDS
DEPARTMENT OF GEOLOGICAL SCIENCES
UNIVERSITY SOUTHERN OF CALIFORNIA
LOS ANGELES, CALIFORNIA
90089-0741
(213) 743-2920**

NOVEMBER 1, 1987

TABLE OF CONTENTS

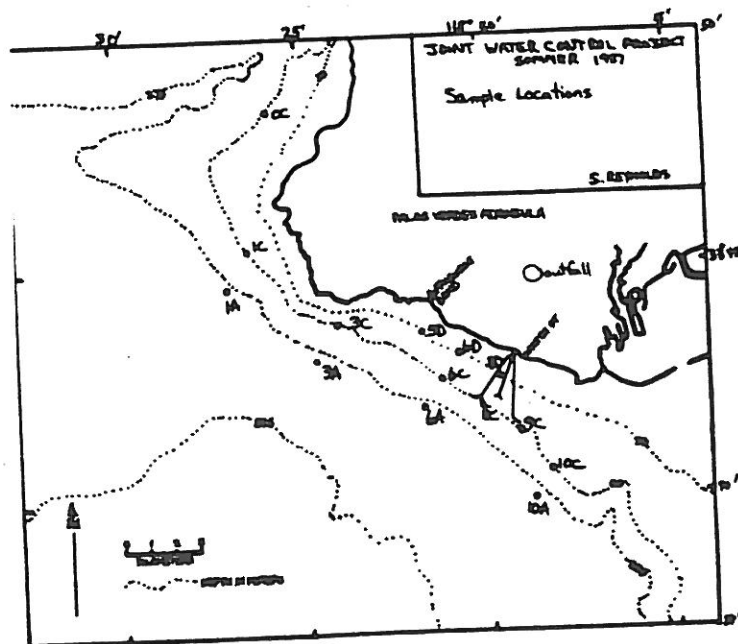
Methods.....3

X-radiography cruise notes.....4
 Description of individual x-radiographs.....5
 Interpretation of stratification seen in x-radiographs.....8

Downcore grain size measures.....9
 Spatial distribution of grain sizes through time.....25
 Downcore grain size distributions.....30

Qualitative description of coarse fractions downcore.....35
 Mineral categories.....36
 Quantitative mineralogy of Palos Verdes Shelf sediments.....37

Mass balances.....49
 Sedimentation rates.....52
 Sediment dynamics on the Palos Verdes Shelf.....54
 Possibilities for exhumation of the buried DDT layer.....56



METHODS

1. Coring was accomplished using the SCCWRP gravity corer aboard the Sea-S-Dee.

2. Subsampling for x-rays: a plastic box (3' long with a cross-sectional area of 2"x3") was intruded into the core before the sample had been removed from the pipe barrel. This sample was sliced and curated, leaving 1-3 samples per core, each sample having a maximum length of 1' and cross-sectional area of 3" x 10/16".

3. X-radiography was accomplished using a Hewlett Packard oven-type x-ray at 4.5 kV, 2.8 mA power. Sample was laid directly on the film, yielding a true-scale image. Exposure time was automatic.

4. Grain size distributions were measured using pipette (for the less than 63 micron fraction) and settling tube (for the greater than 63 micron fraction) methods. For samples 8C and 8D, part of the coarse fraction consisted of light-weight organic material which was not suitable for settling tube analysis. The sand and gravel portion of these samples were determined using standard sieve analysis. In the 1985 study, the operator used a different method, attempting to remove this material by flotation prior to analysis.

5. Mineralogy of the fine and very fine sand fraction of these samples was determined by optical examination under a 40X binocular microscope. Samples were representatively split and at least 300 grains were identified to yield a 95% confidence level.

6. Time lines for cores were drawn based on examination of x-radiograph stratification, down-core grain size distributions, coarse-fraction mineralogy, and DDT and trace metal down-core concentrations. In several sections of the following discussions, I have drawn maps labelled as "pre-discharge" and "maximum discharge". The values used for drawing these maps are taken from the following core depths:

Maximum discharge:

| | | | |
|----------|----------|--------|----------|
| 3A 4-6 | 6A 6-8 | 1C 4-6 | 3C 16-18 |
| 6C 24-26 | 8C 28-30 | 9C 4-6 | 10C 2-4 |
| 5D 14-16 | 6D 12-14 | | |

Pre-discharge:

| | | | |
|----------|---------|----------|----------|
| 1A 4-6 | 3A 8-10 | 6A 14-16 | 10A 6-8 |
| 0C 8-10 | 1C 8-10 | 3C 38-40 | 6C 54-56 |
| 9C 14-16 | 10C 6-8 | 6D 40-42 | 8D 50-52 |

X-RADIOGRAPHY CRUISE NOTES

| STATION | ORIGINAL LENGTH | FINAL LENGTH | COMMENTS |
|---------|-----------------|--------------|---|
| 1C | ? | 21 | |
| 2D | no sample | | coarse sandstone, mostly shell fragments. Core washed out twice, so just took grab from core catcher. |
| 2C | 34 | 29 | live worms & tubes on surface. |
| 2A | 29 | 29 | gastropod |
| 3A | 34 | 32 | clam. Discarded 0-2 cm sample. |
| 3B | 20 | 20 | lots of clams. |
| 3C | 47 | 40 | |
| 3D | 24 | 27 | shell hash at bottom |
| 5D | 40 | 37 | |
| 5C | 57 | 45 | Core catcher sample fell out. |
| 6C | 46 | 43 | |
| 7C | 52 | 44 | |
| 6A | 29 | 29 | |
| 6B | 34 | 32 | |
| 8A | 36 | 33 | |
| 8B | 23 | 22 | |
| 8C | 48 | 45 | |
| 8D | 33 | 19 | couldn't subsample whole core (ie..this is not all compaction). |
| 9C | 28 | 25 | |
| 10A | 26 | 22 | |
| 10B | 25 | 24 | |
| 10C | 25 | 23 | First 2 drops only got large shells. Took grab sample of those. |
| 10D | 48 | 44 | |

DESCRIPTION OF INDIVIDUAL X-RADIOGRAPHS

2A:

Sample coarsens upwards. Faint branching burrow at the top of the core is post-retrieval.

- 0-4 Low density sandy mud. Fairly sharp lower boundary.
- 4-10 Medium density mud. Gradual lower boundary.
- 10-17 Higher density mud. Some disruption? Gradual lower boundary.
- 17-27 Higher density mud. Gradual lower boundary.
- 27-32 Laminated muds.

3A

Sample fines upward. Low-density areas at 17-21 cm are artifacts.

- 0-7 Low density mud with scattered clams. Sharp lower boundary.
- 7-16 Medium density mud. Gradual lower boundary.
- 16-30 Higher density mud. Gradual lower boundary.
- 30-32 Laminated mud.

6A

Faint branching burrows near the top are post-retrieval. The larger burrow between 6-12 cm may be natural.

- 0-6 Low density mud. Sharp lower boundary.
- 6-14 Medium density mud. Gradual lower boundary.
- 14-21 Higher density mud. Gradual lower boundary.
- 21-30 Laminated sandy mud.

8A

Large meandering burrow is post-retrieval.

- 0-7 Low density mud with medium-size shells. Sharp lower boundary.
- 7-13 Medium density mud. Gradual lower boundary.
- 13-20 Higher density sandy mud. Gradual lower boundary.
- 20-33 Gradually increasing density.

10A

- 0-4 Low density mud with scattered grains (probably small shells. Sharp lower boundary.
- 4-22 Gradually increasing density.

3B

- 0-10 Low density mud with clams. Some of the faint branching burrows here are post-retrieval. Sharp lower boundary.
- 10-22 Higher density sandy mud.

6B

- 0-19 Low density mud with clams. Many of the faint branching burrows are post-retrieval. Sharp lower boundary.
- 19-32 Higher density mud.

8B

Blob at 15-17 cm is an artifact.

0-11 Low density mud with clams. Lowest density material is from 7-11 cm. Sharp lower boundary.

11-22 Higher density sandy mud.

10B

0-3 Low density mud. Gradual lower boundary.

3-24 Higher density sandy muds. Gastropod at 16 cm.

1C

There appears to have been some disturbance during coring and/or subsampling, but beneath that, I believe that I can see stratification that is being disrupted by bioturbation. The base of the post-1956 deposit is difficult to place, could be at 8 or 14 cm. Most of the small, faint branching burrows are post-retrieval, but medium-diameter burrows extending to the top appear to be real. The dark blob from 9-14 cm is an artifact.

2C

The core sample at present time has many small surficial burrows which don't show up in the x-ray. The faint, large-diameter burrows between 4-7 cm may be real.

0-15 Low density mud with clams. Lowest density from 10-15 cm. Sharp lower boundary.

15-22 Medium density mud. Gradual lower boundary.

22-29 Higher density mud.

3C

Beneath the large gastropod at 6-7 cm is a hole 3 cm long caused by the cutting wire pulling the gastropod up. Faint branching burrows in 0-10 cm are post-retrieval. Other blotches and blobs are artifacts.

0-21 Low density mud with clams. Sharp lower boundary. Some stratification at 2.5-3, 5-6, and 8-9(?) cm. These could represent storm deposits.

21- Higher density mud.

5C

The lower x-radiograph has large dessication cracks.

0-31 Low density mud. Possibly some stratification at 4-4.5 cm. Faint branching burrows may be natural. Sharp lower boundary.

31-45 Higher density sandy mud.

6C

Faint branching burrows in the upper radiograph are post-retrieval.

0-35 Low density mud. Sharp lower boundary.

35- Higher density mud.

7C

- 0-35 Low density mud with scattered shells. The faint branching burrows at the top right don't show up on the core surface, but are probably post-retrieval. Very-high density layers at 19 and 31 cm are problematic. Sharp lower boundary.
- 35-44 Higher density sandy mud.

8C

- No burrows on the surface of the core. The cone-shaped area along the right at 25-37 cm is an artifact.
- 0-27 Low density mud. Sharp lower boundary.
- 27-45 Higher density mud.

9C

- Faint branching burrows not seen on surface of core.
- 0-14 Low density mud. Lowest density at 5-11 cm. Sharp lower boundary.
- 14-25 Higher density mud.

10C

- 0-4 Very low density mud. Sharp lower boundary.
- 4-19 Low density mud with concentrations of very large shells at 8-9, 11-14 cm.

3D

The blob at 7-10 cm is probably not real. Fining upwards deposit of coarse granules, lending a grainy texture to the x-ray.

5D

Also a fining-upwards deposit. The shell at 22 cm is disarticulated. Stratification at 9 cm is between two fining-upwards deposits.

8D

- 0-9 Low density mud. Sharp lower boundary.
- 9-14 Mud and coarse vegetative material.
- 14-19 Rounded granitic cobbles (pipe ballast) encased in low-density mud.

10D

- 0-19 Low density mud. Fairly sharp lower boundary. This is too thick in this area to be related to effluent discharge. Probably comes from harbor material.
- 19-44 Laminated sandy mud with shells. Resembles storm deposits.

INTERPRETATION OF STRATIFICATION SEEN IN X-RADIOGRAPHS

The stratification seen in stations at the 30-m isobath is mostly related to storm deposition. The exception is at 8D. The lowest layer there is ballast material for the pipeline. The intermediate layer is near-field effluent material (1937-1956?). The upper layer is a mixture of nearshore sediments and far-field effluent material.

The upper layer of low-density mud at stations along the 60-m isobaths represent the post-1956 deposit (Fig. 1). The exception is 10C, where the upper layer may represent only an ephemeral deposit which is periodically swept away. Other stratification seen in stations from the western edge of the shelf is probably related to storm deposition.

The upper layer of low-density mud at 300-m isobath stations represent the post-1956 deposit. At station 6A, the two upper layers are interpreted to represent the post-1956 deposit, based on examination of the grain-size data. Other deeper layers in the 300-m isobath stations are related to longer-term changes in the depositional systems of the PV shelf.

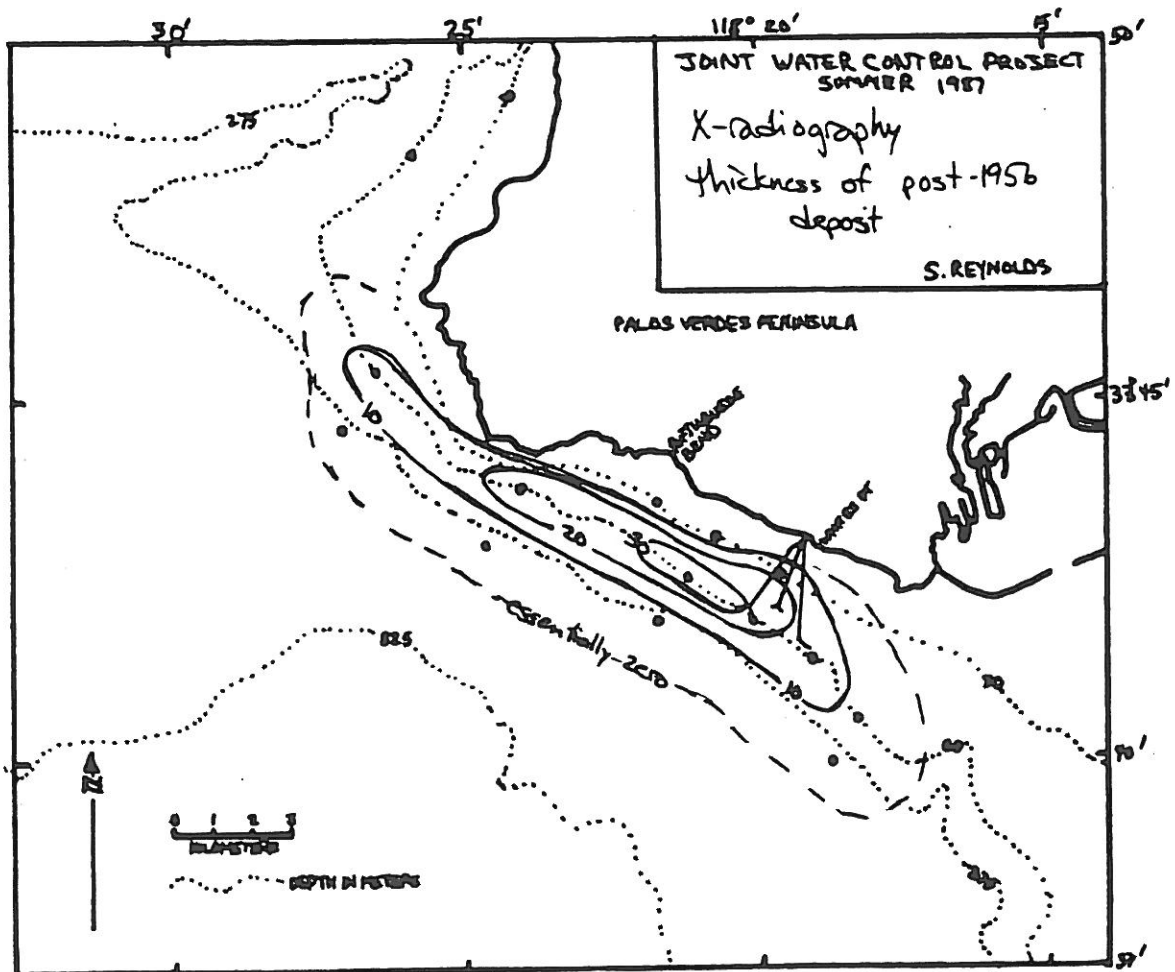


Figure 1

DOWN-CORE GRAIN SIZE MEASURES

0C (fig. 2)

The mean grain size of 5-5.2 phi is fairly stable downcore. Sorting is good downcore. Percent sand increases by 3% downcore at the expense of silt and clay, but no obvious explanation for this subtle trend.

1C (fig. 3)

7 cm = 1970; 14 cm = 1956.

Mean phi shows finest sediments at time of maximum discharge and at present. This fining is caused by an increase of clay relative to silt; percent sand is fairly uniform downcore. Sediments which are highest in clay are also the most poorly sorted, suggesting that these layers have undergone the least amount of storm reworking.

3C (Fig. 4)

2 cm = 1985; 17 cm = 1970; 28 cm = 1956; 38 cm = 1937.

Mean grain size shows a very jagged pattern. In general, sediments are coarsest at the bottom, fine upwards to a peak at 17 cm, then coarsen upwards. Shorter-term deviations, on the order of 1/2 phi, are superimposed on this long-term trend; these deviations probably represent increased storm influence on the coarser deposits. The changes in mean grain size are caused by changes in the percentages of all three fractions (sand, silt, and clay), except during peak discharge times, when percent sand is at a stable minimum. Shorter-term deviations are mostly the result of changes in the relative amounts of silt and clay; percent sand changes on a more gradual scale, reflecting major changes in the rate of effluent discharge only. The intervals 2-4 cm and 6-8 cm are positively identified as storm deposits through correlation with x-radiography stratification and mineralogy; these layers have increased sand relative to clay, and are generally better-sorted. The upper 2 cm contains much finer sediments than those immediately downcore, as a result of increased clay relative to sand. These 2 cm have been deposited since 1985 and we have had no major storm since; these could reflect sediments which have not yet been reworked.

6C (Fig. 5)

2 cm = 1985; 27 cm = 1970; 43 cm = 1956.

This core shows a remarkably gradual change in sediment size through time, with very few short-term deviations. At the bottom of the core, mean phi is relatively coarse; it fines to a peak at 27 cm, then coarsens to 4 cm, then fines upward from there. Percent silt is fairly stable downcore; percent sand mirrors, in the opposite direction, mean phi. The most dramatic changes (and the only high-frequency variation) is in % clay. Only pre-1956 sediments have good sorting; finer sediments are more poorly sorted. As in 3C, sediments deposited since 1985 are relatively finer and could represent yet-to-be-reworked deposits.

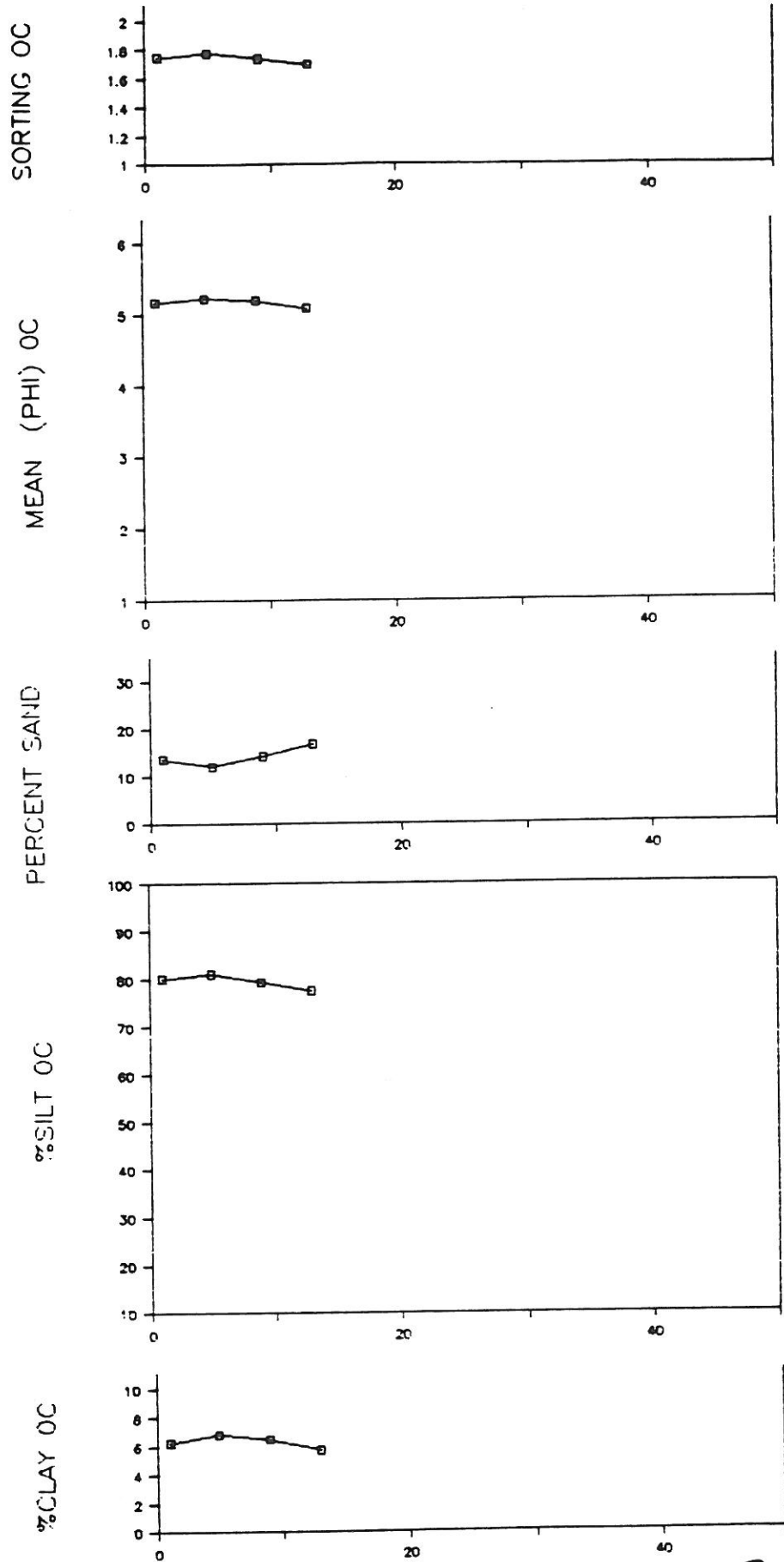
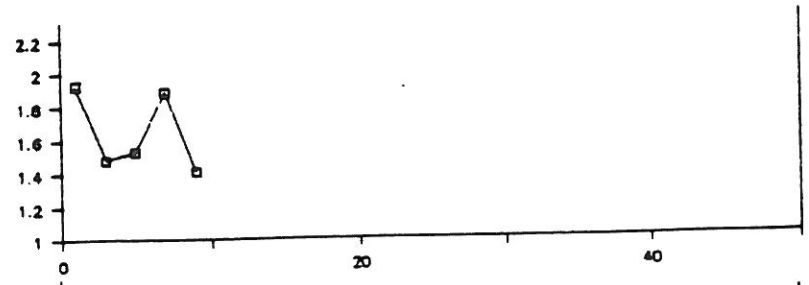
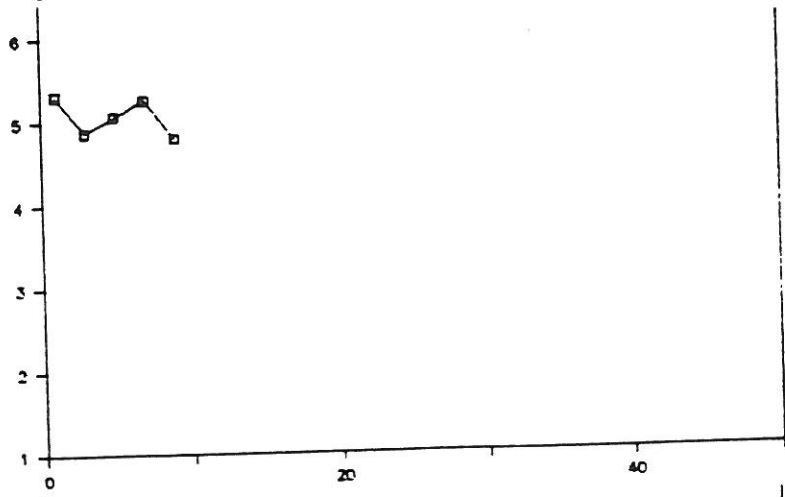


Figure 2

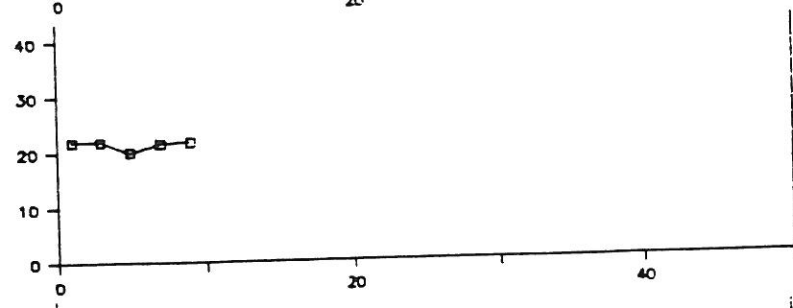
SORTING 1C



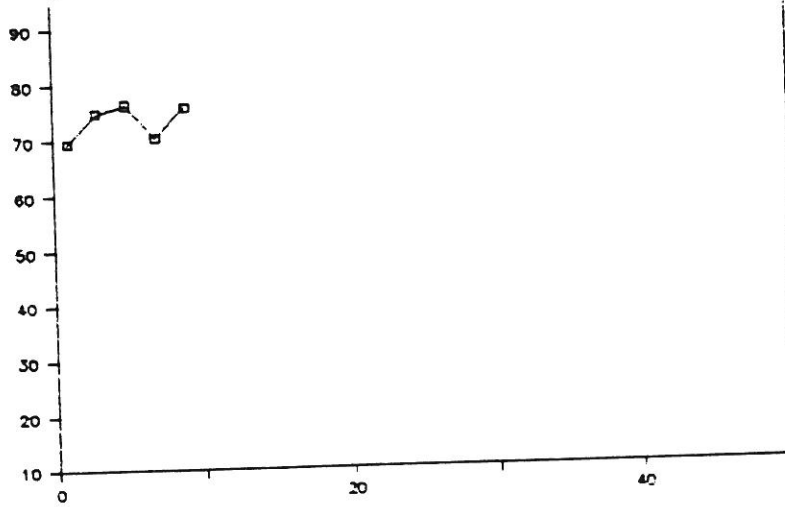
MEAN (PHI) 1C



PERCENT SAND



%SILT 1C



%CLAY 1C

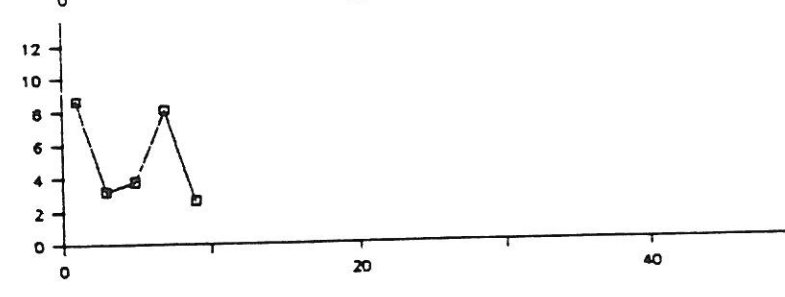
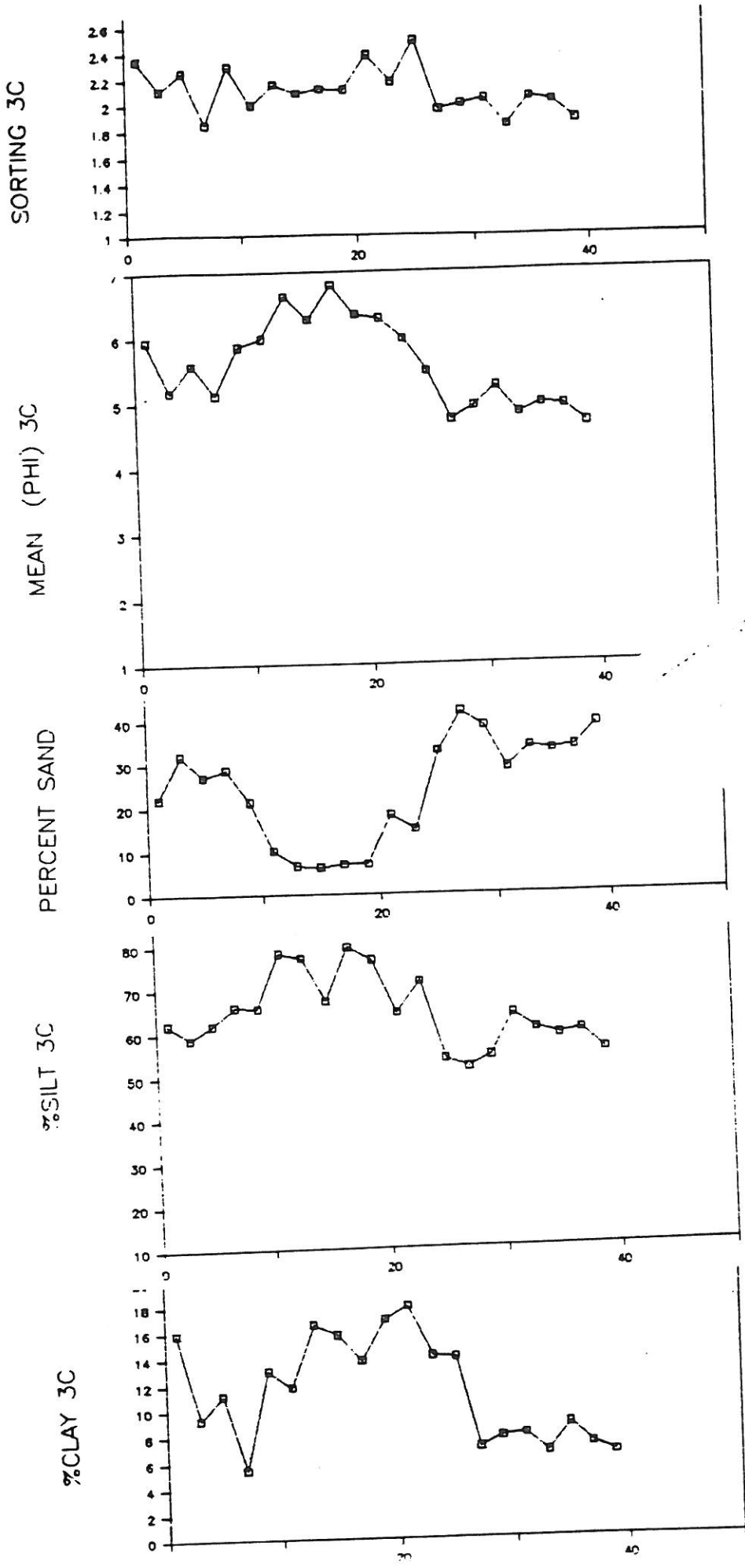


Figure 3



39

Figure 4

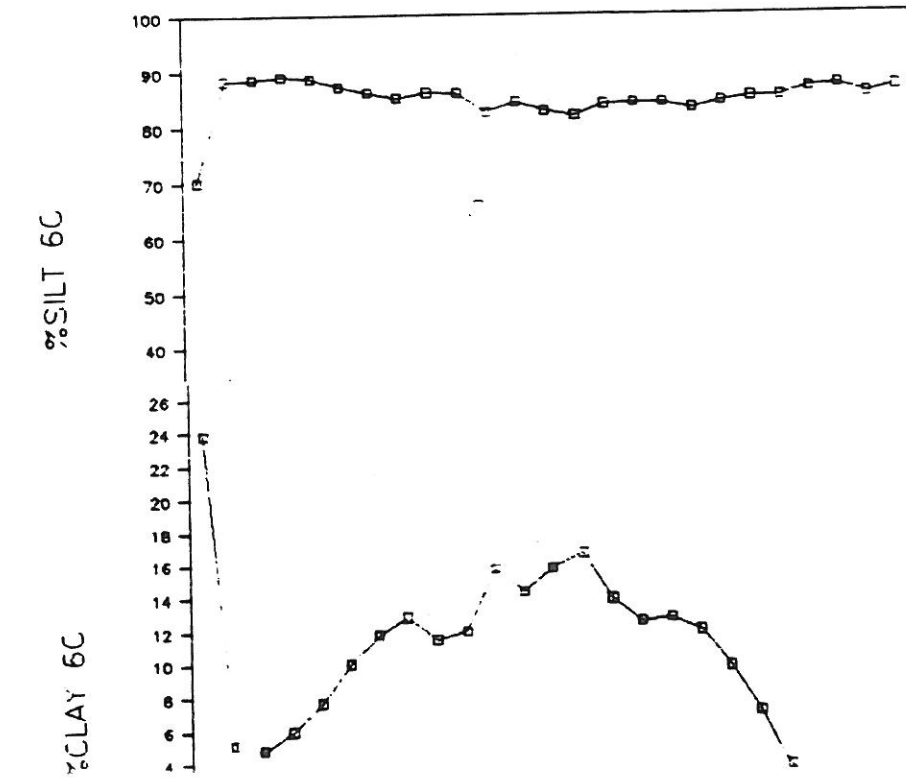
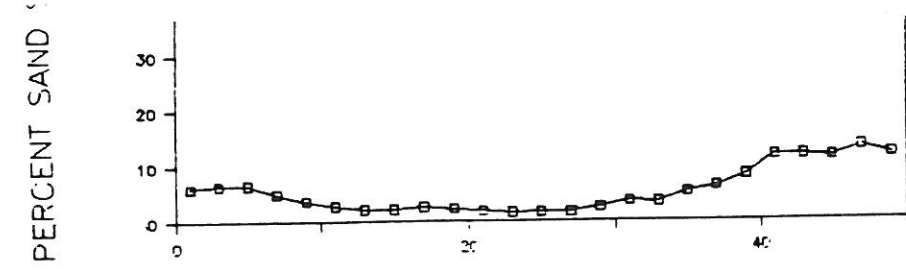
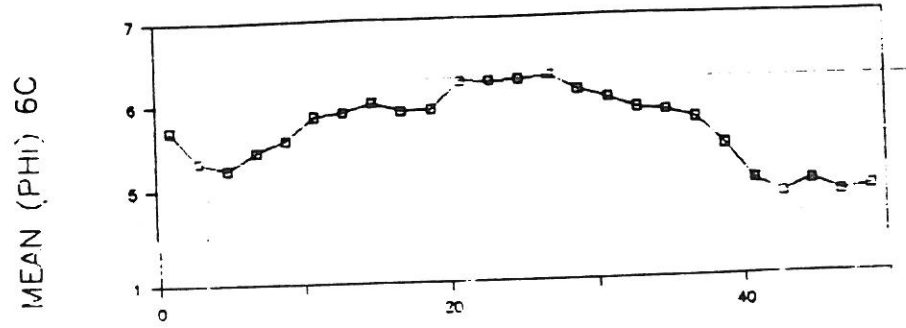
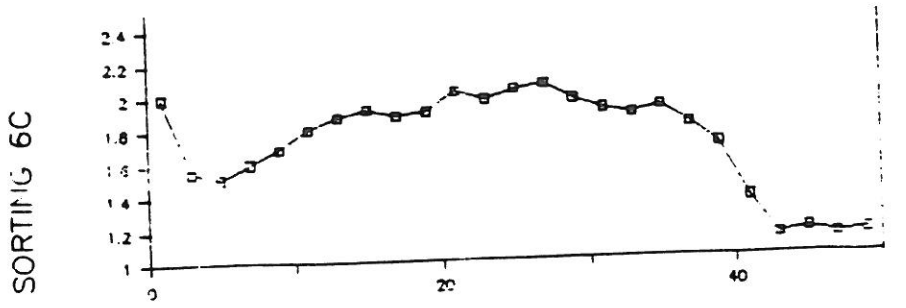
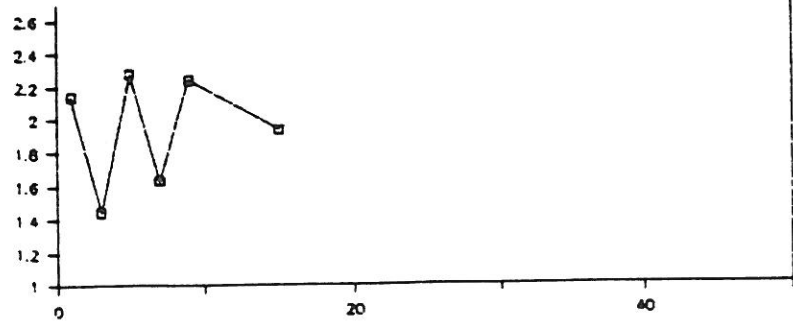
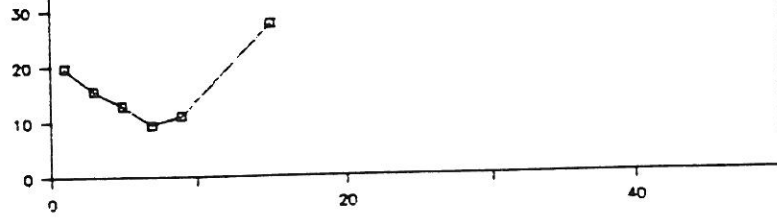
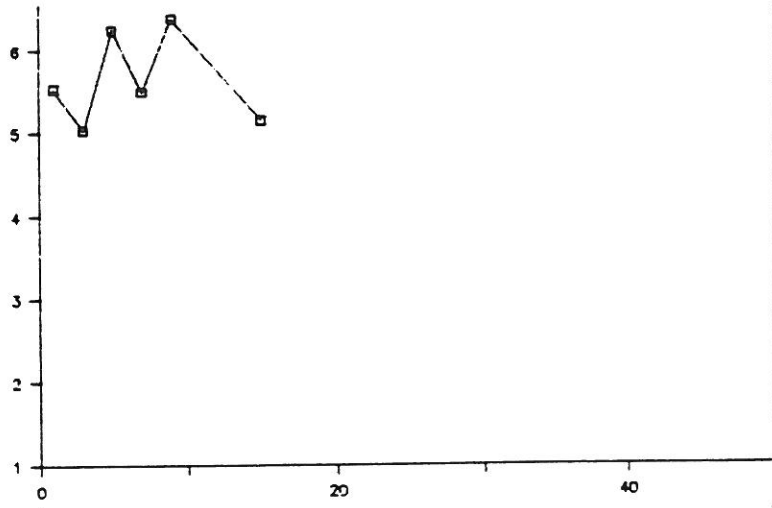


Figure 5

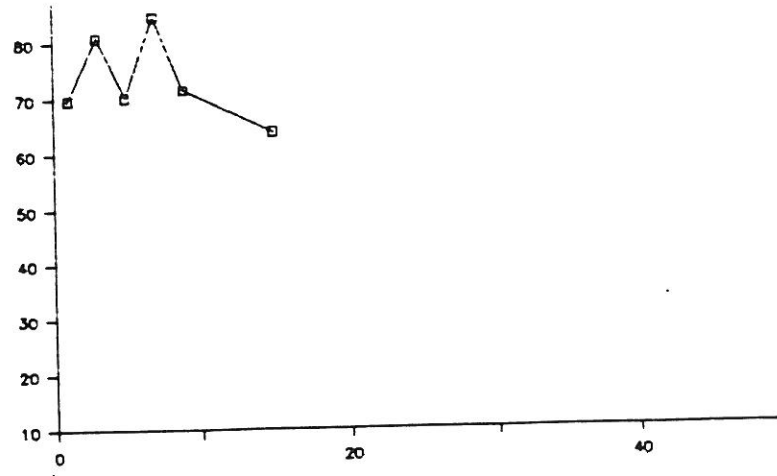
SORTING 9C



MEAN (PHI) 9C



%SILT 9C



%CLAY 9C

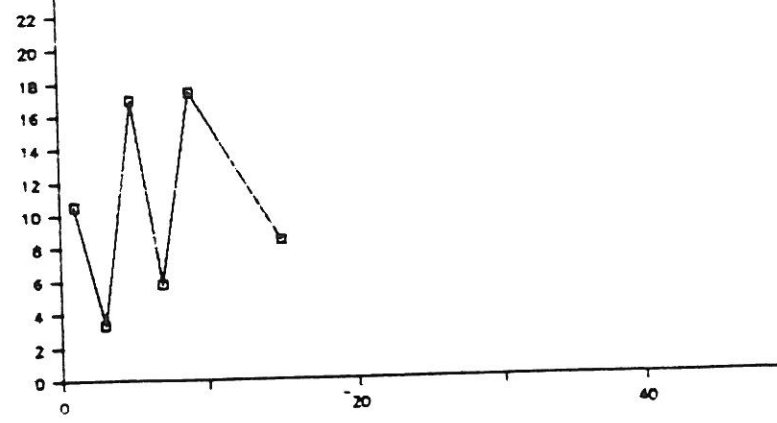


Figure 7

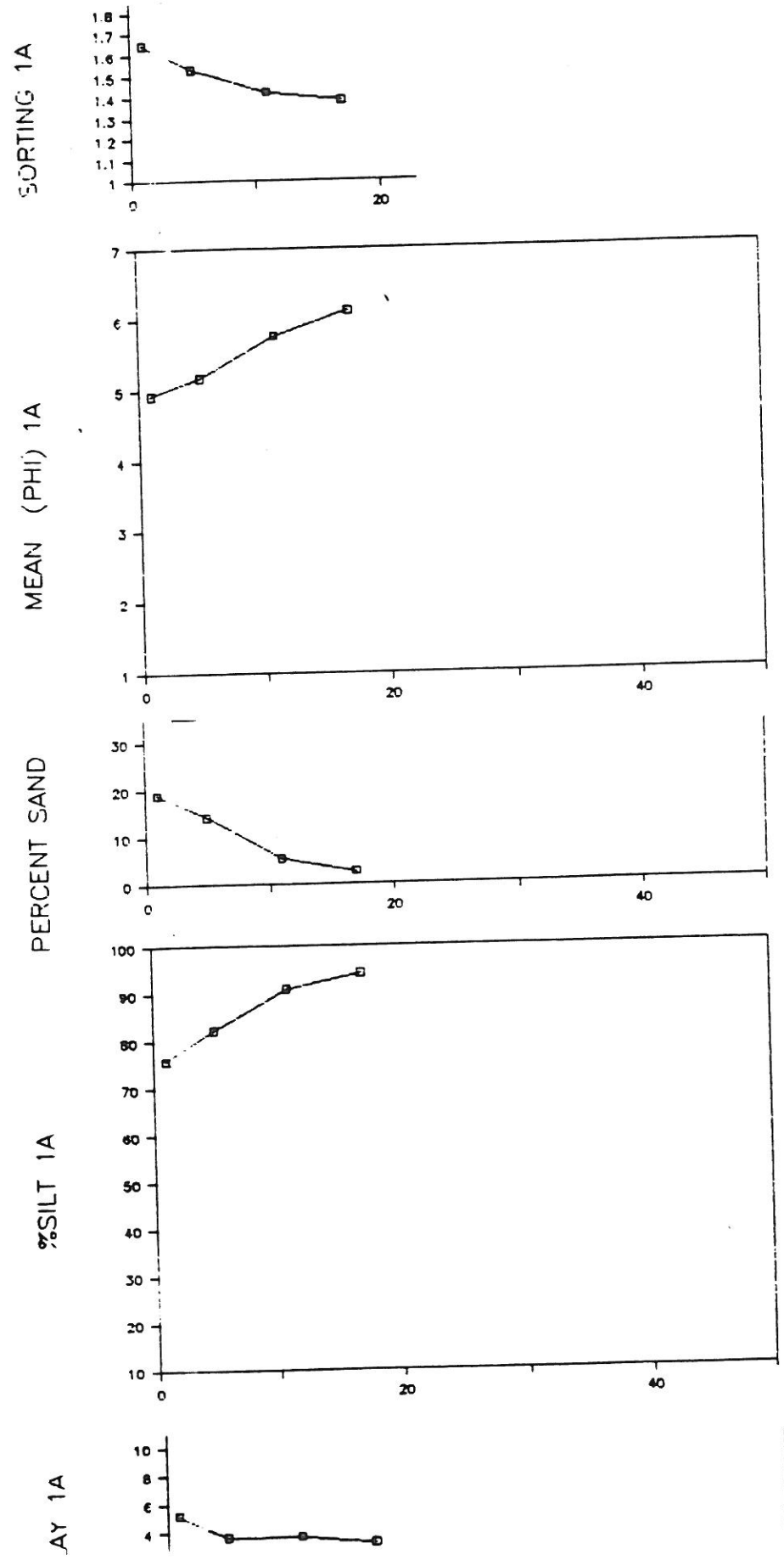
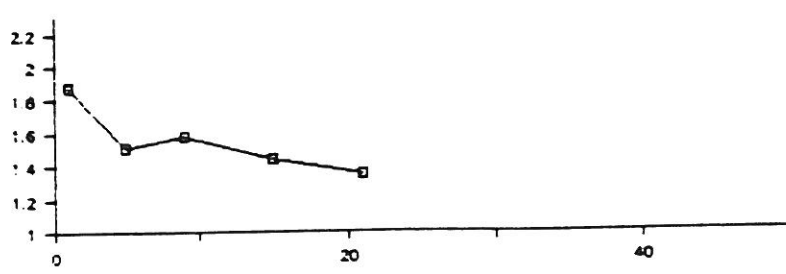
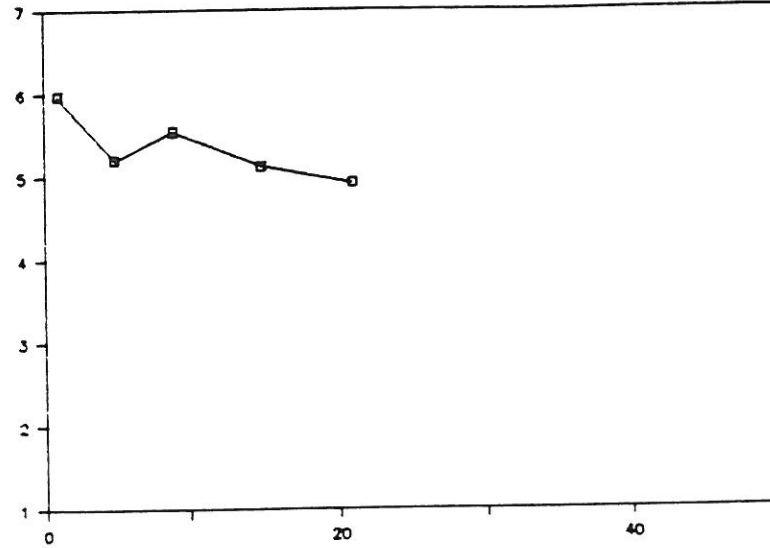


Figure 8

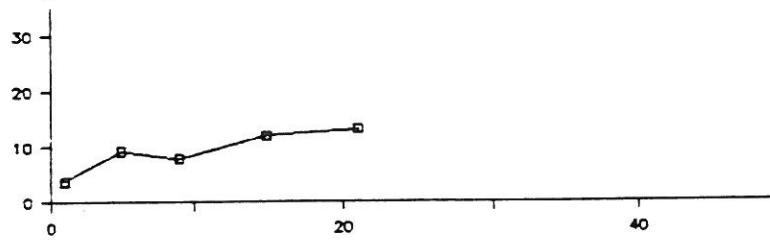
SORTING 3A



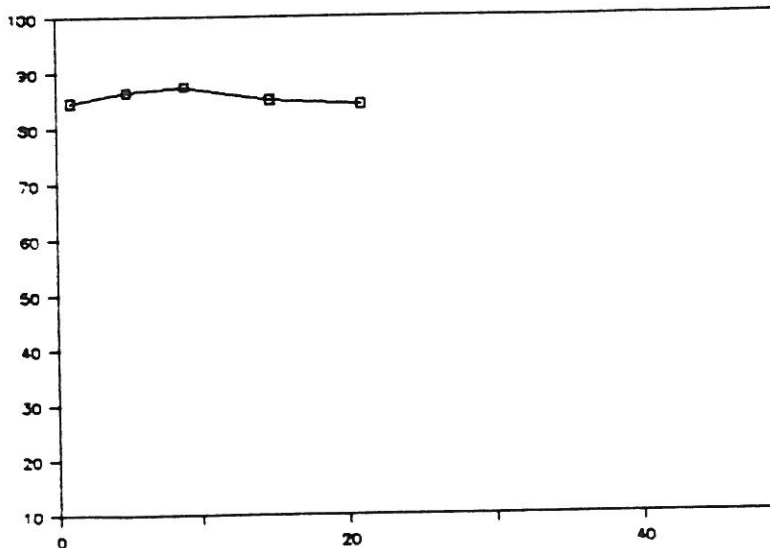
MEAN (PHI) 3A



PERCENT SAND



%SILT 3A



%CLAY 3A

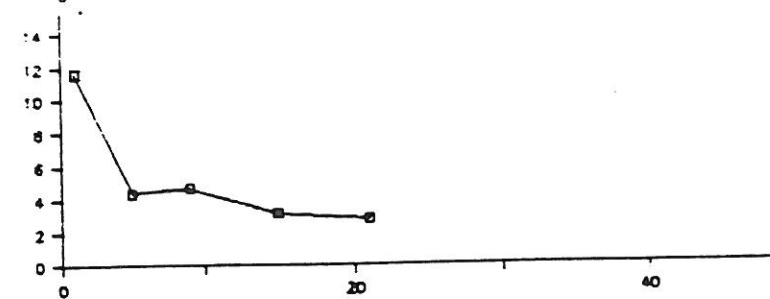
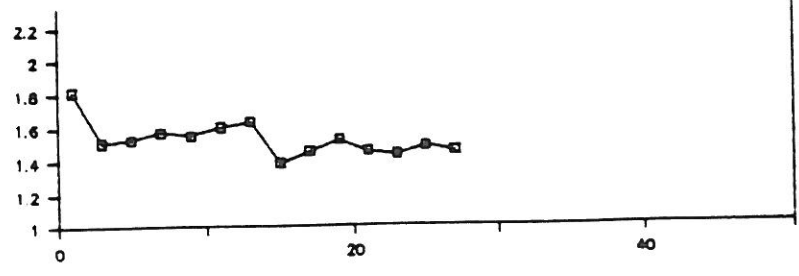
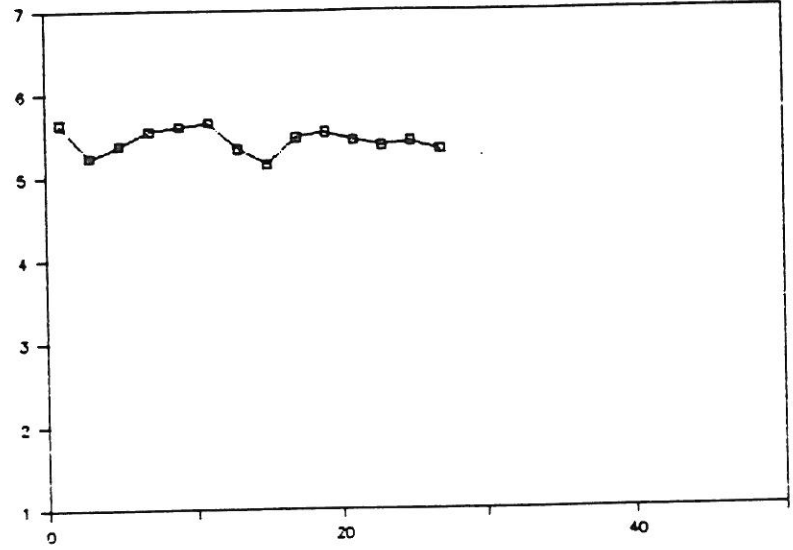


Figure 9

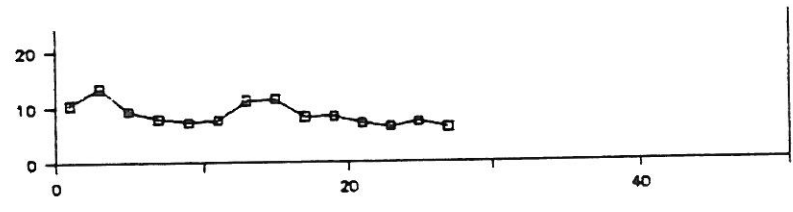
SORTING 6A



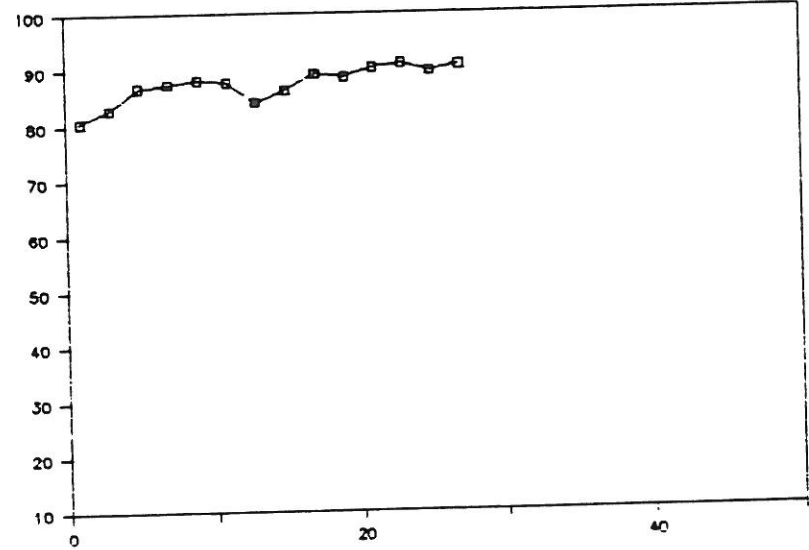
MEAN (PHI) 6A



PERCENT SAND



%SILT 6A



%CLAY 6A

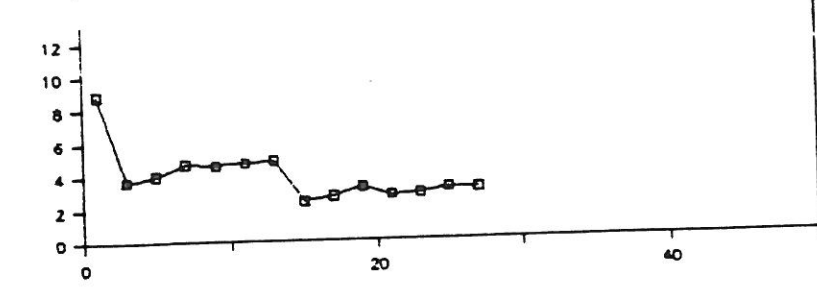


Figure 10

10A (Fig. 11)

4 cm = 1956.

Only the uppermost sample is affected by effluent discharge. The long-term trend is coarsening upwards caused by an increase in sand relative to silt. Apparently the effluent discharge has had little affect on this long-term trend.

5D (Fig. 12)

Three fining-upwards cycles are present, 30-24, 24-7, and 7-0 cm. The trends in mean phi are reflected by changes in all three fractions. Sorting is very poor throughout, and finest material is the most poorly sorted. In all likelihood, these represent deposits of material derived from erosion of the PB slide during storms. Since a very large amount of material was eroded during the 1983 storm, I would say that 7-24 cm represents the deposit of that event.

6D (Fig. 13)

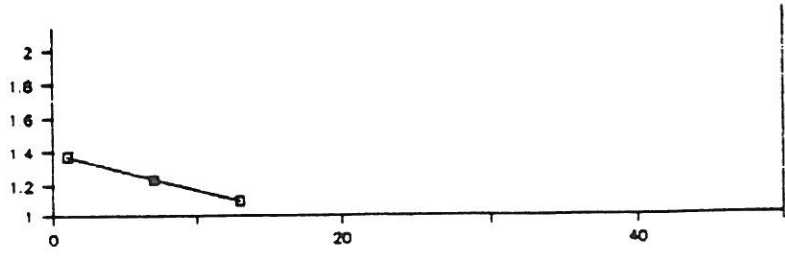
Gradual fining-coarsening trends which involve only very small changes in the percent of sand, silt, and clay are present. These probably represent the far-field deposits of the material eroded from the PB slide.

8D (Fig. 14)

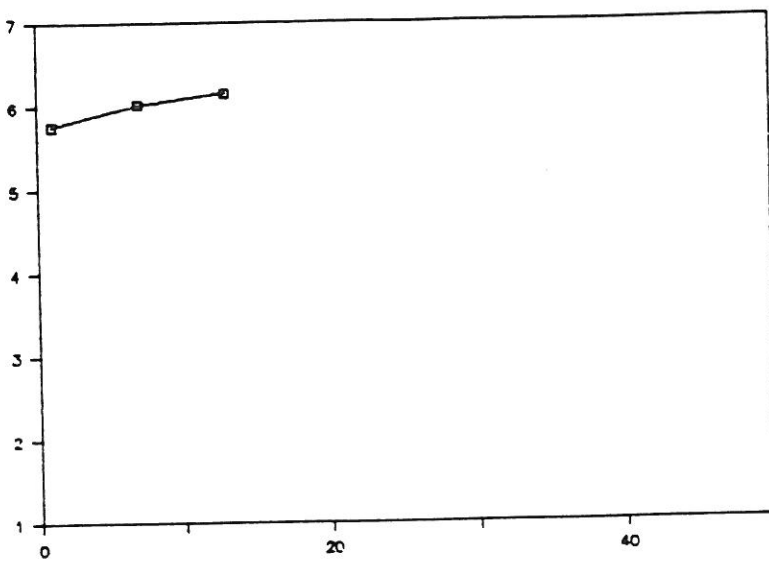
Between 38 and 19 cm lies a fine peak which is rich in vegetative material. Since this material is so similar to what is present at 8C today, I feel that this probably represents material deposited between 1937-1956 when the outfall was discharging directly into this location. However, ballast for the pipeline underlies this deposit on the x-radiograph sample. If this is ballast laid down for the 1937 pipeline, the above interpretation is probably correct. If this is ballast laid down for the later pipelines, then the data should be re-interpreted. Above 19 cm, sediments show a typical fining-coarsening upwards trend reflecting changes in the rate of outfall discharge from 1956-1985. In this interval, percent silt increases and then decreases upwards, and sand shows the reverse trend. The percent clay shows a more erratic trend, probably as a result of storm winnowing.

In the x-radiograph core, vegetative material lies between 10-14 cm, and rocks are encountered at 14 cm. The 1985 grain size data shows fine peaks at 6, 10, and 20 cm. Obviously this is a highly variable station. A large part of this variability could be the result of sediment reworking during pipeline construction and maintenance. The pipeline itself could cause perturbations in the local current and wave regime, resulting in localized erosion and deposition. Leakage from the pipeline could also influence this area. In the future, I would suggest intense monitoring of a 7D station.

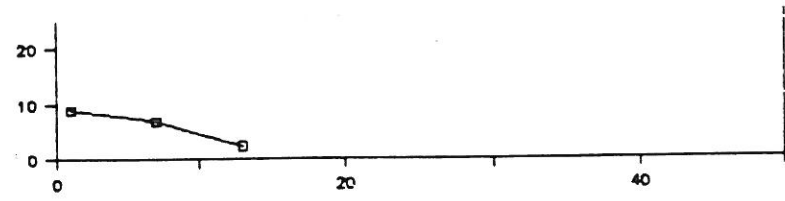
SORTING 10A



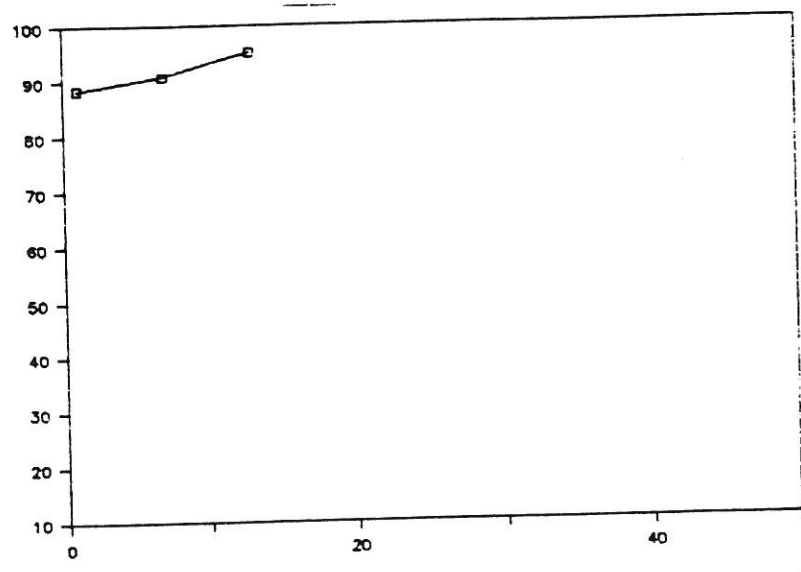
MEAN (PHI) 10A



PERCENT SAND



%SILT 10A



%CLAY 10A

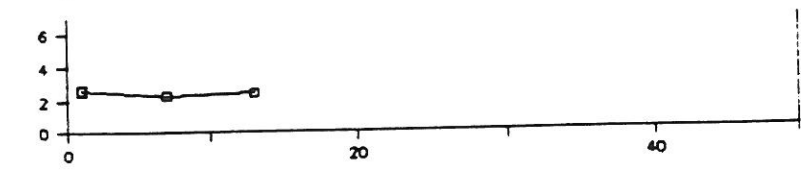


Figure 11

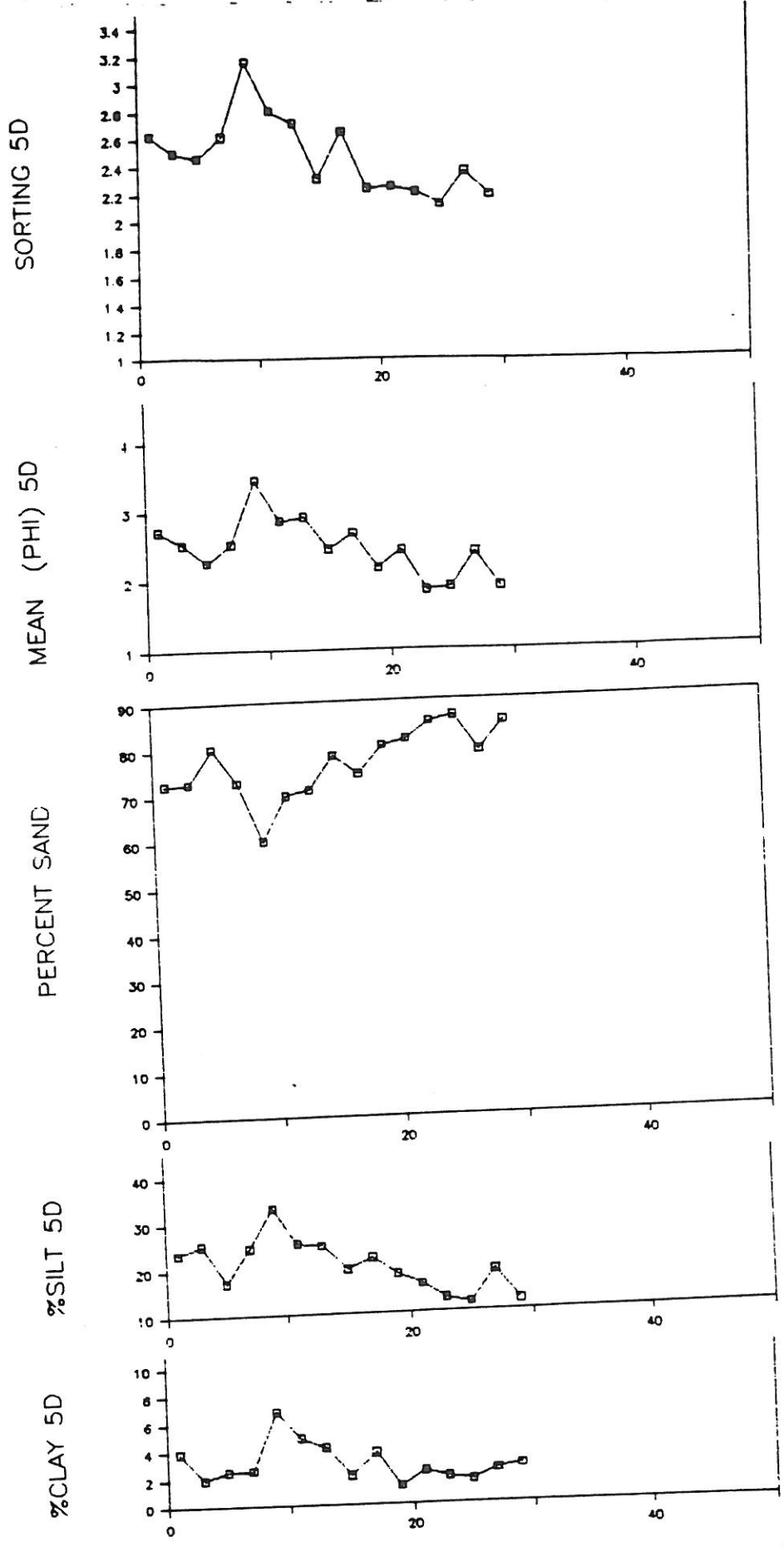


Figure 12

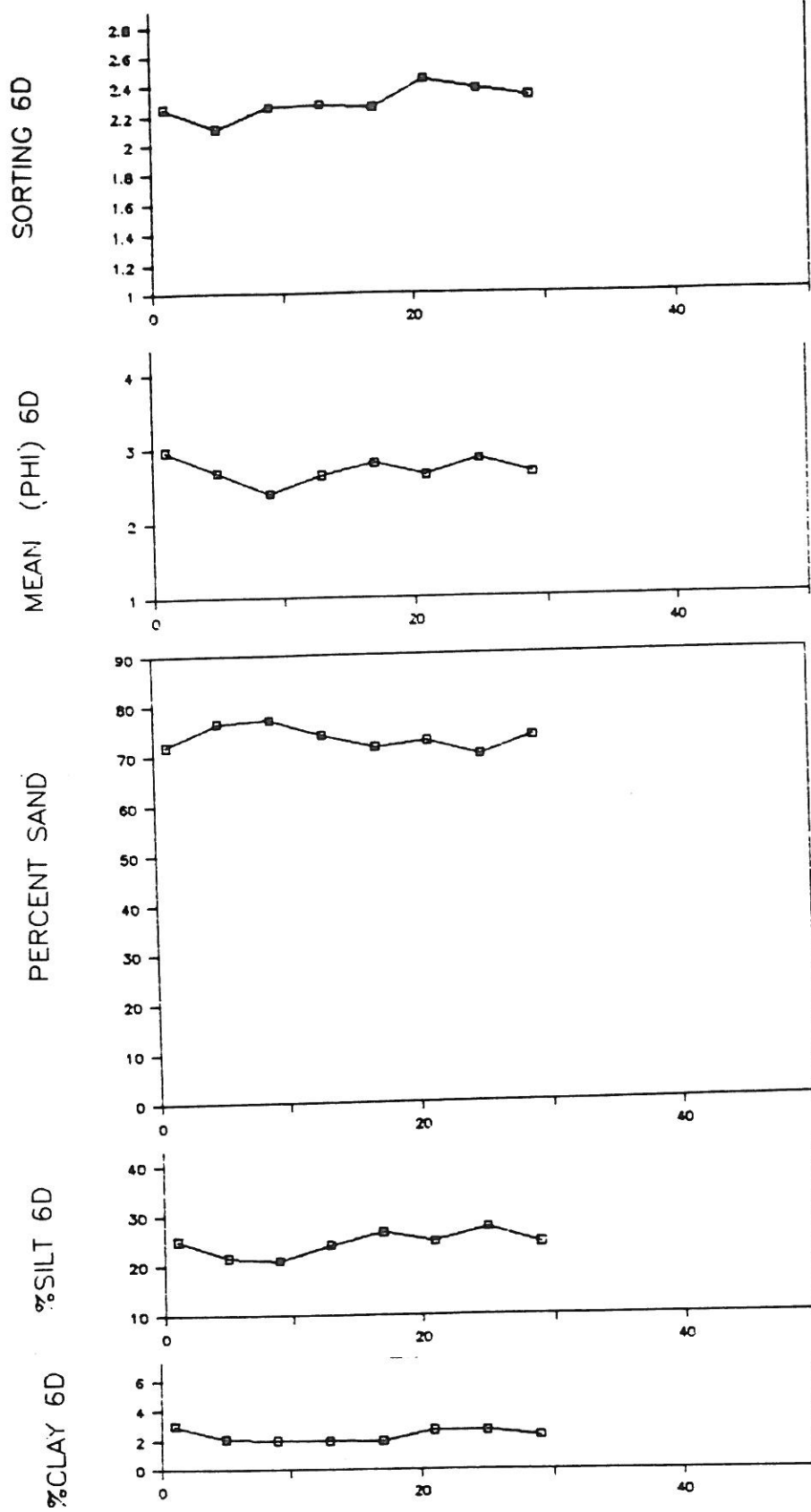


Figure 13

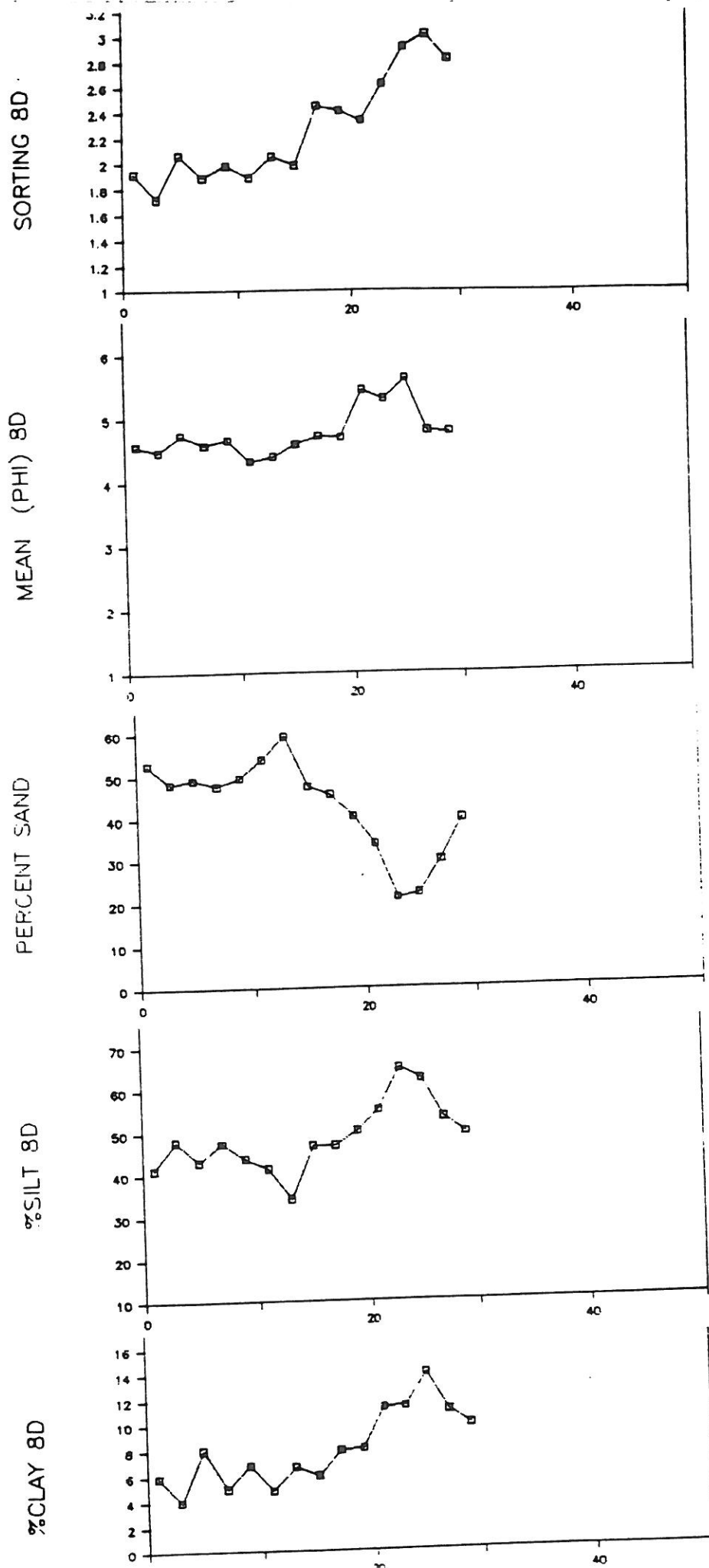


Figure 14

SPATIAL DISTRIBUTIONS OF GRAIN SIZES THROUGH TIME

Mean grain sizes (in phi) clearly show the effect of effluent discharge through space and time. Examining first the map of pre-discharge values (Fig. 15), a simple pattern of fining offshore is found, with finest grain sizes at 10A. During the time of maximum effluent discharge (Fig. 16), the pattern changes dramatically. The simple fining offshore trend is interrupted by a narrow belt of fine material at the 60m isobath, which is replaced by coarser material at the 300-m isobath stations. Present-day distributions (Fig. 17) are intermediate between these two patterns. Isograds "bow out" around the outfall due to finer material in this area, and the area in the central shelf between the 5-6 phi interval is expanded relative to pre-discharge values. However, compared to the time of maximum discharge, today's values on the central shelf are coarser.

Another feature of the present-day distribution is anomalous coarsening at station 10C. Station 10C is in the area of a rock reef which supports a wide variety of hard-substrate benthic animals, as evidenced by fauna in the x-radiograph. Three drops at this station were necessary to retrieve this x-radiograph sample. This station is in the general area of the San Pedro Sea Valley, and the Captain Rusty Walz of the Sea-S-Dee has found episodic strong currents in the area, which may be related to flow down the canyon. Glauconite is present in the coarse sediments. All of this data points to the possibility of erosion at this station.

Present-day distributions of % clay in these sediments (Fig. 18) most clearly show the impact of effluent discharge on the shelf, since the effluent is the primary source of clay-sized material in this area. The highest percent clay is at station 6C, with high amounts all along the 60-m isobath, and decreasing amounts seaward and shoreward. Pre-discharge sediments show percent clay smoothly increasing offshore. Percent silt (Fig. 19) shows a gradual increase offshore, with the 40 and 60% isograms bulging shorewards near White's Point, meaning that station 8D has a higher percentage of silt than stations at similar water depths and distances from the shoreline. Percent sand (Fig. 20) shows the inverse -- gradually decreasing offshore. Closely-spaced gradients between the nearshore and the outfall reflect the low percentage of sand in the effluent. Anomalously high percentages of sand are present at station 10C.

Standard deviation is a measure of the amount of sorting of grain sizes. Higher standard deviation mean more poorly sorted sediments. In this area, all sediments are poorly sorted due to 1) the mixing of sediments from numerous sources; 2) the offshore introduction of sediments whose particle sizes may not be at equilibrium with energy levels at that water depth; and 3) local input of relatively immature, poorly sorted sediments at the shoreline. The distribution of present-day values of sorting (Fig. 21) shows central shelf values between 2-2.5, with sorting increasing both seaward and shoreward. The most poorly sorted sediments are at station 5D, reflecting input of very poorly sorted sediments from the PB slide.

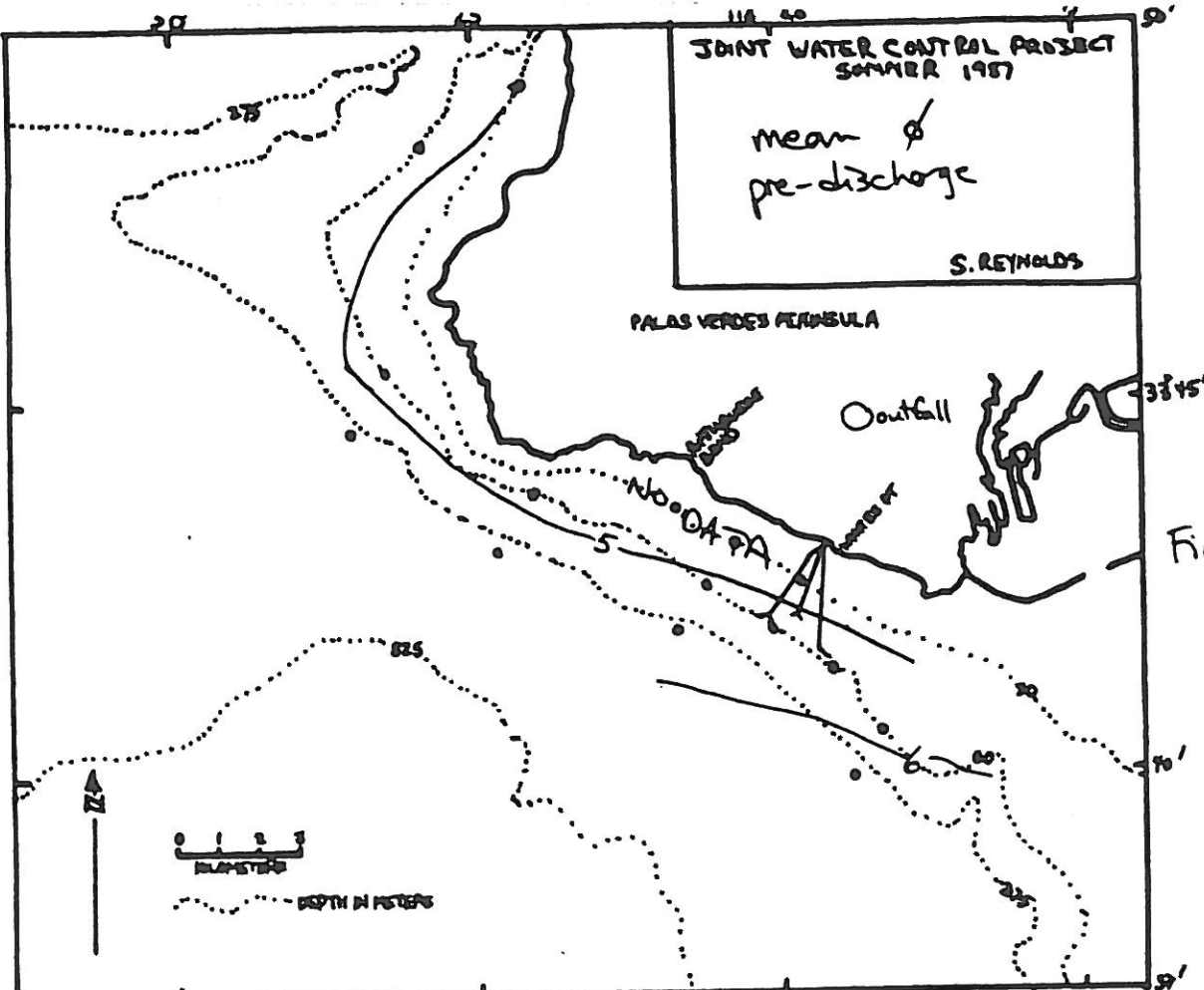


Figure 15

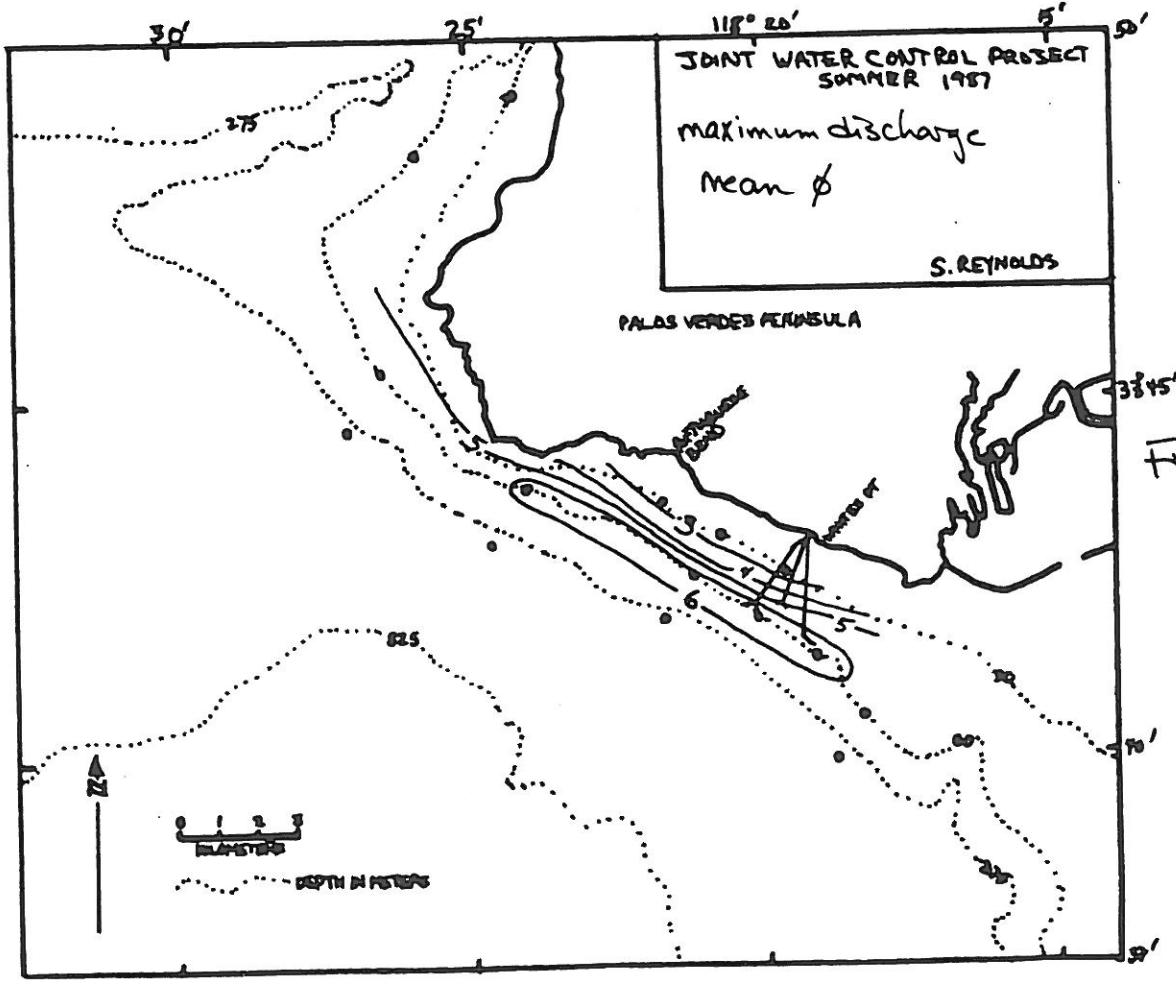


Figure 16

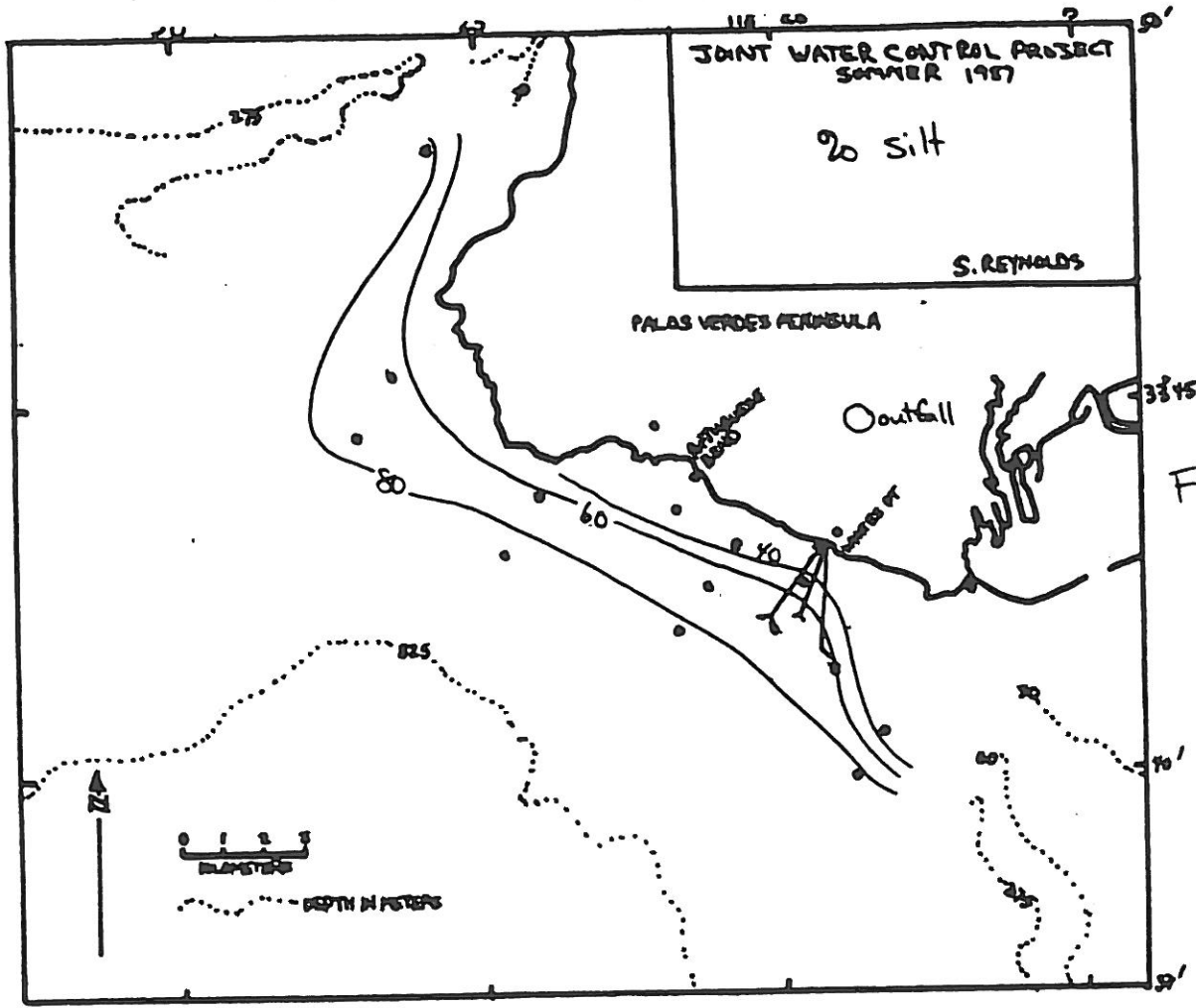


Figure 19

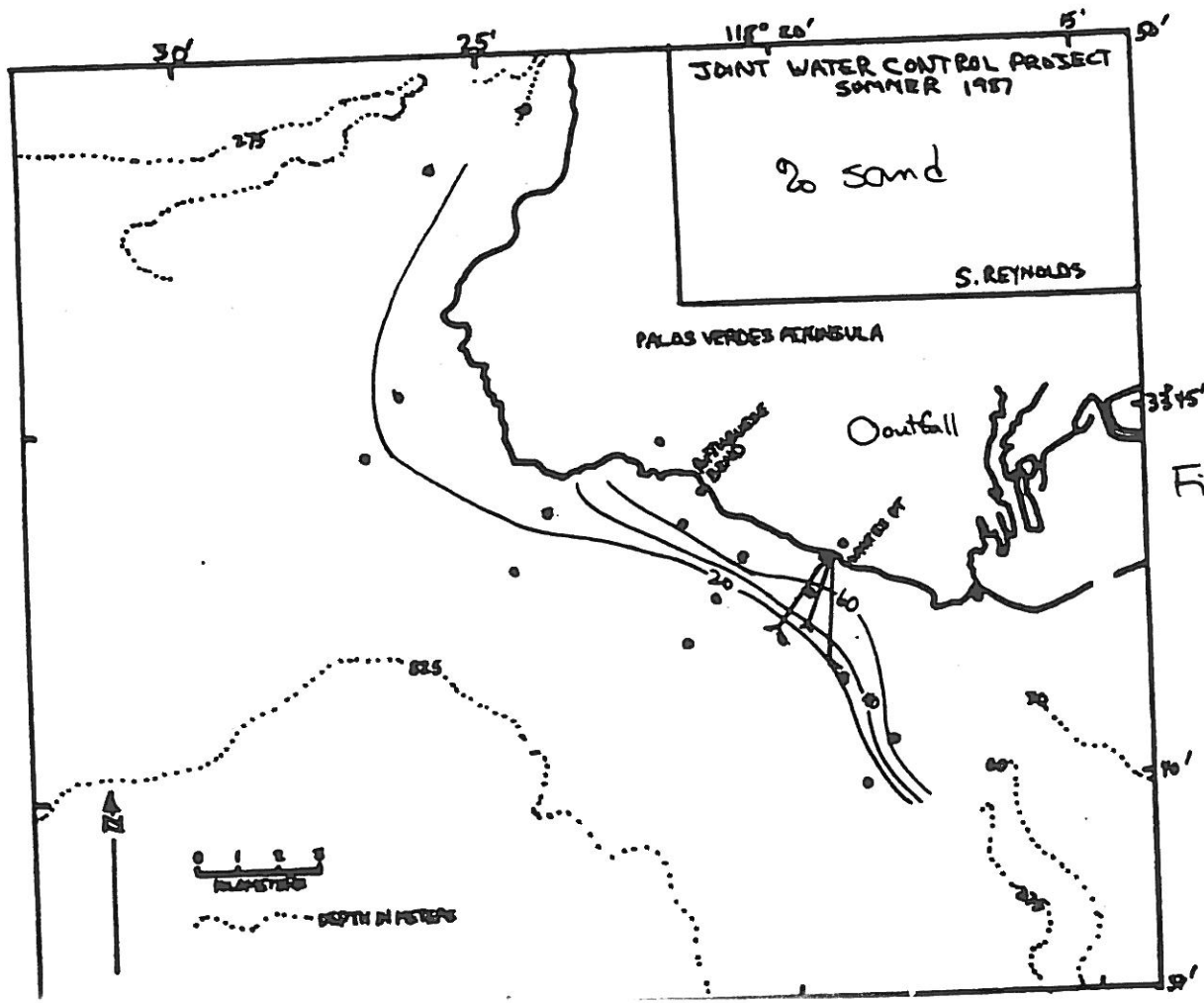


Figure 20

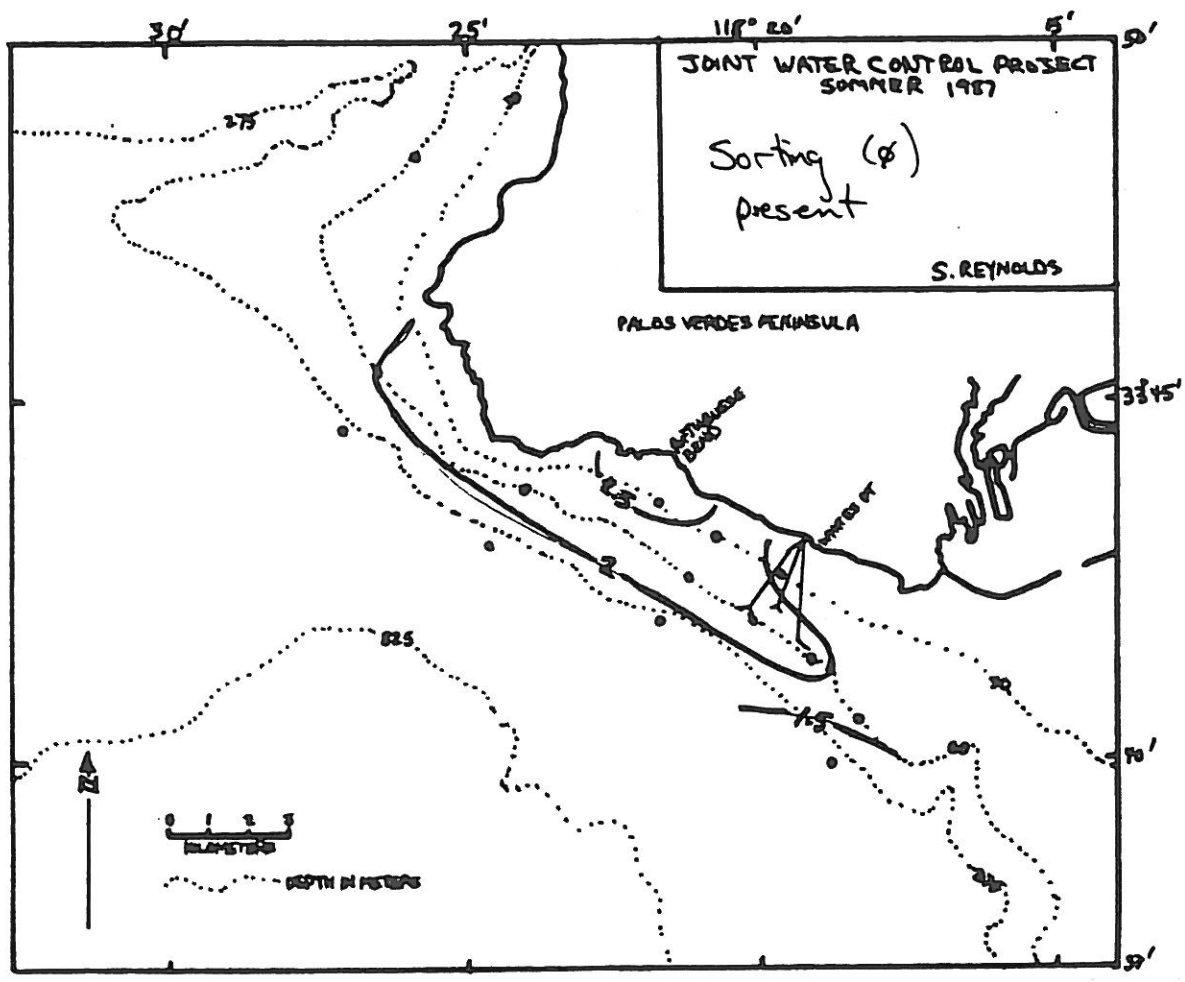


Figure 21

DOWNCORE GRAIN SIZE DISTRIBUTIONS

An examination of the complete grain-size distribution gives a more detailed understanding of the changes in these sediments through time. Moment measures assume that a given population of grains should approach a normal distribution, and they measure the population's deviance from the norm. Another theory holds that any natural sediment is actually composed of several normal populations, the overlap of which creates a non-normal distribution. The separation of these populations is an involved, tedious process, but I have tried to make rough estimates of these populations using a graphic-fit method, which has been illuminating if not quite precise. I will discuss these for only a few stations.

The sand and silt fractions at station 6C (Fig. 22) generally separate into two (roughly) normal distributions, with 1-3 smaller normal populations in the fine silt and clay fractions. The two of interest are: a broad curve with a peak at 5.5 phi and a better-sorted curve peaking at 4.5 phi. The 4.5 phi curve dominates the distribution at the bottom and the top of the core. The 5.5 peak dominates in the central part of the core during periods of maximum discharge. The peaks in the fine silt and clay range also show a systematic change with depth, increasing in size during periods of maximum discharge.

My initial interpretation of this data was that the 4.5 peak represented natural sediments washed into the area during storms and that the broader curve at 5.5 phi represented effluent material. However, after I completed the mass balance-sedimentation rate analysis, I realized that natural sediments, on the average, could only account for 10% of the total post-1956 deposit at this station. The area encompassed by the 4.5 phi curve represented 39% of the total post-1956 deposit. Working with the same type of relationships on the grain-size distributions of other cores, I was unable at any point to define a normal population which encompassed a percentage of the sediment which was close to what the percentage of natural sediments should have been at that station.

The alternative explanation is that these subpopulations represent not different sources, but different processes. The 4.5 peak curve represents sediments (both natural and effluent-derived) which had been reworked or deposited during storms. This premise explains the very well-sorted nature of this subpopulation. The increasing dominance of the 4.5 peak upwards in the core as effluent discharge rate decreased, is also rational: as the total sedimentation rate decreases, the influence of storm reworking increases. During periods of maximum discharge, storm reworking would have relatively less influence on the rapidly growing sediment pile, if storm reworking affects only the uppermost part of the sediment pile.

Other stations close to the outfall display similar

Station
bc

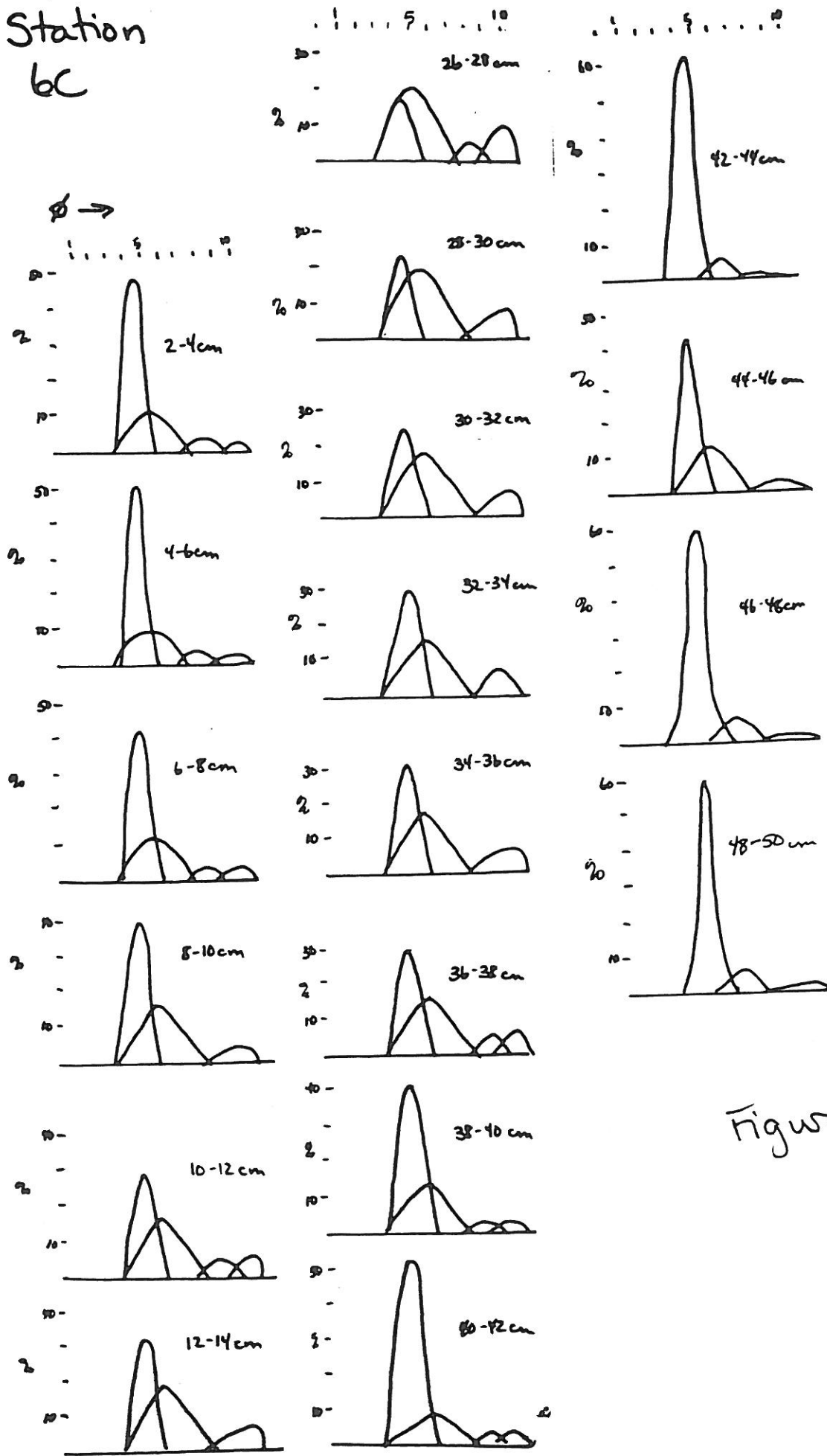


Figure 22

patterns. Station 8C (Fig. 23) is another interesting example. The dominant curve peaks at 5.5 phi; several populations exist in the fine silt and clay fractions, and a broad distribution exists in the fine to coarse sand range which represents vegetative material. During times of maximum discharge, these are the only populations present in the distribution. Going both above and below peak discharge times, a well-sorted subpopulation appears in the 4.5 phi range. This population increases in importance upwards, and represents 30% of the population at the 0-2 cm interval. Since it is unlikely that 30% of the surficial sediment at the outfall is non-effluent, this relationship reinforces the claim that this subpopulation represents storm reworking.

At station 1C (Fig. 24), all grain size distributions are dominated by a well-sorted subpopulation peaking at 4.5 phi. Apparently, the low sedimentation rate in this area allows for almost complete reworking of the slowly-growing sediment pile. A subpopulation peaking at 3.5 phi is also present; this material must be locally derived but shows no systematic change in its relative importance downcore.

The percentage of the sediment which is within this well-sorted subpopulation, then, can be taken as a rough measure of the amount of storm reworking of the sediment. There does seem to be a correlation between sedimentation rate and the average percentage of this population (Fig. 25). A rough-fit correlation, extrapolated to the 0% reworking index, suggests that at sedimentation rates higher than 2 cm/year, storms will have virtually no affect on the sediment. Actually, the curve is probably a logarithmic relationship since storms, if they occur, will always have some affect. But this number leads to an interesting conclusion: that storms probably only affect less than the upper centimeter of sediment at any given location.

Station 8C

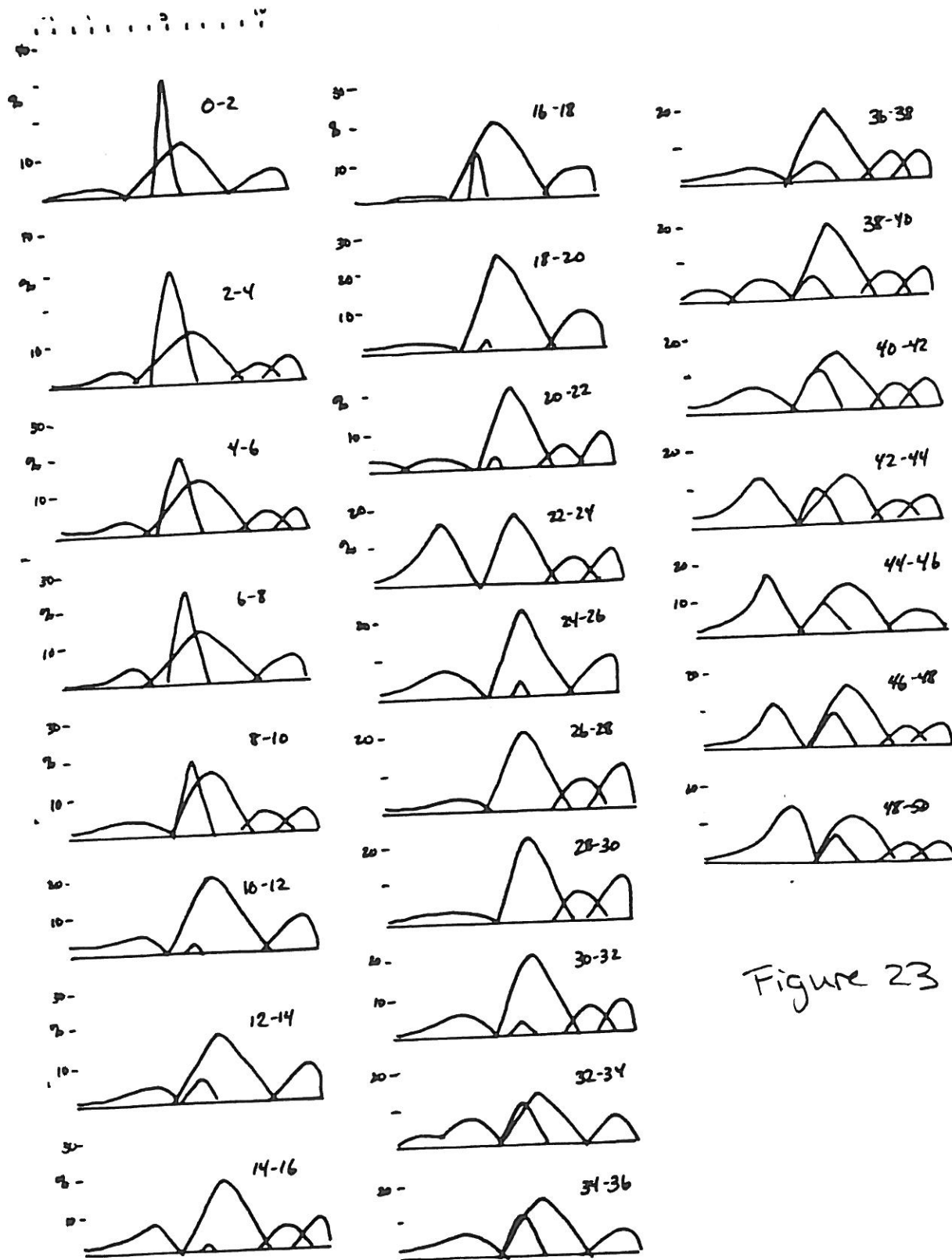
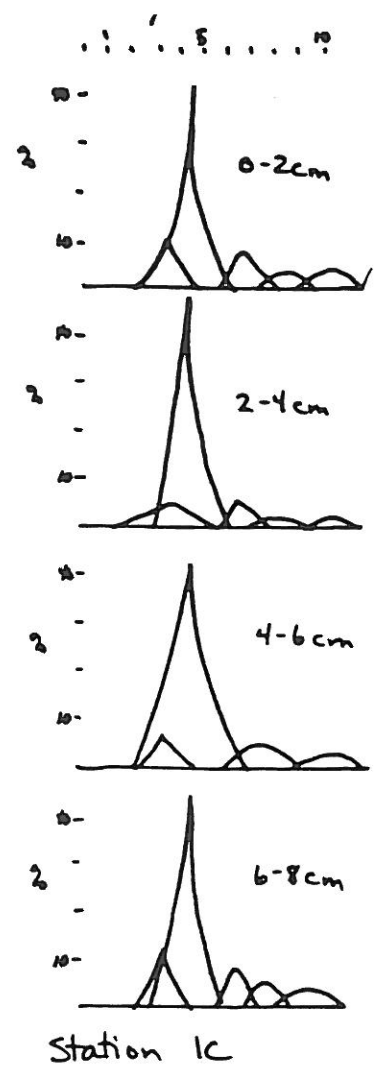


Figure 23



Station 1C

Figure 24

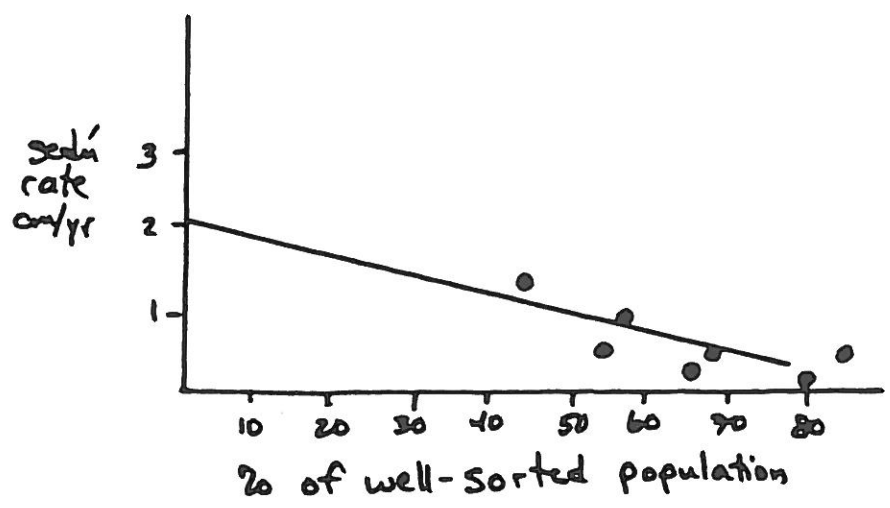


Figure 25

QUALITATIVE DESCRIPTION OF DOWNCORE COARSE FRACTIONS

In order to get a rough idea of downcore and spatial distributions of mineralogies, I first visually examined the entire coarse fraction.

6A

0-26 Fine grained terrigenous sand with fibers.

10A

0-12 Fine grained terrigenous sand with glauconite.

0C

0-12 Fine grained terrigenous sand.

1C

0-2 Fine grained terrigenous sand, similar to 0C.

6-8 Same, with addition of vegetative material.

3C

0-10 Mostly fine-grained terrigenous sand with some fine-grained vegetative material.

10-12 Sharp decrease in total sand. Increasing proportion of vegetative material relative to terrigenous sand.

12-22 Small amount of sand. Vegetative material about 50%.

22-24 Decreasing amount of vegetative material.

24-26 Sharp increase in amount of terrigenous sand.

26-30 About 10% vegetative material.

30-32 Increase in vegetative material.

32-40 Mostly fine-grained terrigenous sand.

9C

0-2 Very micaceous fine-grained terrigenous sand.

4-10 Same, with addition of medium-grained vegetative material.

14-16 Increased amount of terrigenous sand, but still minor amounts of vegetative material.

5D

0-28 Brownish-colored rock fragments (medium sand)

Carbonate fragments (coarse sand)

6D

0-30 Medium-grained brownish-colored rock fragments.

Very dissolved and pitted carbonate fragments.

8D

0-16 Mostly fine-grained terrigenous sand, with smaller amounts of coarser particles composed of seeds, shell fragments and rock fragments. Amount of vegetative material increasing downwards.

16-18 Moderately sharp increase in vegetative material, with a corresponding decrease in terrigenous sand.

18-22 Vegetative material increasing at expense of fine terrigenous sand.

22-30 90% vegetative material.

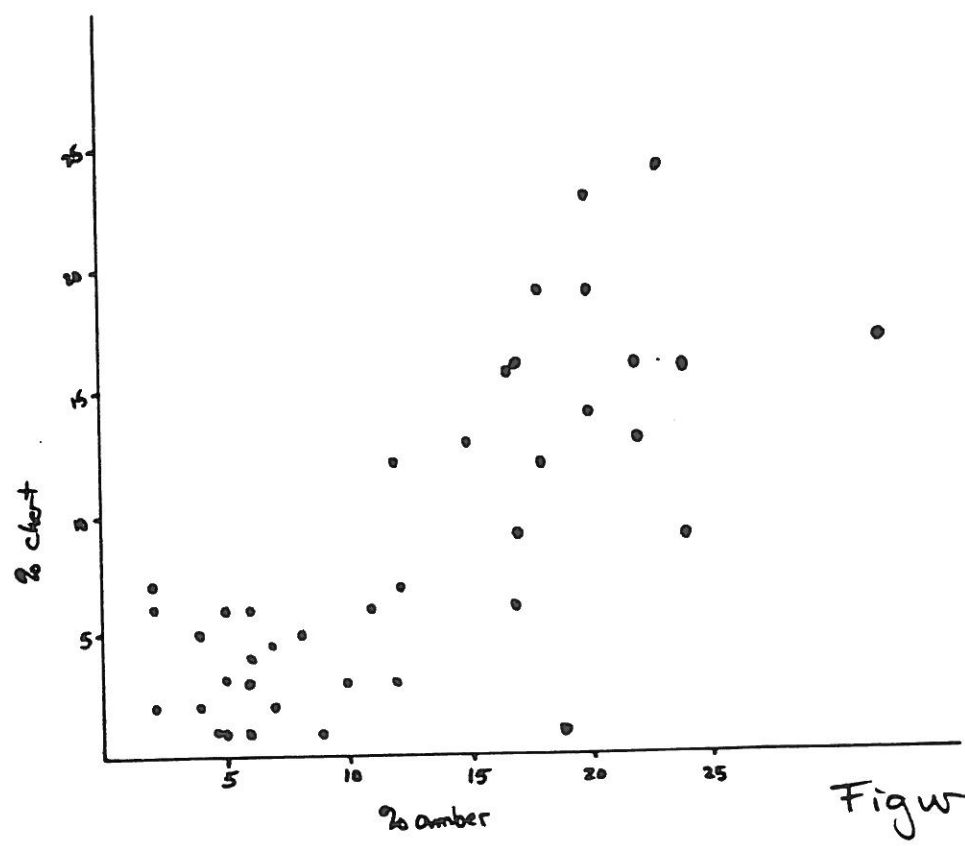
MINERAL CATEGORIES

- 1. Organic material: cellulose, chitin, fibers, seeds, spores, resin, and petroleum.
- 2. Shells: fresh and old, carbonate and siliceous.
- 3. Epidote: characteristic greenish-yellow color, lacking well-developed cleavage. Source is probably LA River/San Pedro Shelf.
- 4. Hornblende: dark green to brown, strong pleochroism, rounded to short prismatic habit. Several sources, local & distant.
- 5. Pyroxene: brown with a pinkish tinge, translucent, biaxial positive. Source is Altamira Shale.
- 6. Glaucophane: blue to violet, strong pleochroism. Includes other blueschist minerals. Source is the blueschist arenite facies of the Altamira Shale.
- 7. Chlorite: green mica flakes.
- 8. Biotite: brown mica flakes.
- 9. Muscovite: clear mica flakes.
- 10. Rock fragments: non-sedimentary polymineralic components.
- 11. Chert: includes porcelanite and possibly some quartzite, dolostone. Mostly reddish-brown to yellow-brown, some beige to white; grey in 10C.
- 12. Quartz: counted as separate varieties--
 - Clear, monomineralic.
 - Cloudy.
 - Amber, translucent.
 - With inclusions (magnetite, rutile, graphite)
 - Other -- smoky, rose quartz, etc...
- 13. Feldspar. Mostly white, opaque. Did not differentiate species.
- 14. Shale/tuff. All fine-grained sedimentary rock fragments.
- 15. Black minerals. Mostly magnetite.

QUANTITATIVE MINERALOGY OF PV SHELF SEDIMENTS

Quartz, in its several species, is the dominant component of all samples. Chert, amber-colored quartz, and clear monocrystalline quartz are the three dominant species. The percentages of these species, within each samples, have been recalculated to 100% and plotted on a triangular graph (Fig. 26). This method of plotting the data clearly separates the samples into two main groups: those with high amounts of clear quartz, and those with intermediate quantities of all three varieties. Percentages of chert and amber quartz show a positive correlation to each other (Fig. 28) showing that they have similar distributions and sources; Percentages of amber and clear quartz vary inversely with respect to each other (Fig. 29), showing that they come from different sources. Clear quartz is a characteristic component of sands coming from rivers which drain granitic source terrains such as the Peninsular Ranges. Three local sources for this species are apparent: sands coming in from the Santa Monica Shelf, which will affect station OC; sands coming in from the San Pedro Shelf, which will affect stations 10A, 10C, and 9C; and the effluent discharge. The ultimate source area for all of these is the Peninsular Ranges. The source area for the chert and amber quartz is the local cliffs of Palos Verdes, which are dominantly Altamira Shale. Since the PB slide also involves Altamira Shale, the mineralogy of sediments derived from the slide will be similar to that of sediments derived from other cliffs. The Altamira Shale does contain some clear quartz, but not in as high an abundance as the three sources mentioned above.

A closer examination of figure (26) displays some interesting relationships between stations. The effluent sample plots near the clear quartz apex. Samples 6C and 8C plot very close to this point, reflecting the dominant influence of effluent sediment at these stations. Samples 9C, 10C, and 10A also plot in this area. These stations receive sediment from both the San Pedro Shelf and effluent, both having high amounts of clear quartz. The local sources of sediment plot further away from the clear quartz apex. Samples from White's Point Cliff, Portuguese Bend slide, and Portuguese Bend beach all have 60-65% clear quartz, with varying ratios of amber quartz and chert. Another group of samples, which are dominantly influenced by local sources of sediment, plot close to these points: 5D, 6D, 3C, 1C, and 1A. This group is offset from the source area towards the effluent values, indicating that effluent is a relatively minor source to these stations. Between the "clear quartz" group and the "local source" group is an intermediate group with Cabrillo Beach, 3A, OC, and 8D. These sediments are drawn from both distant and local sources. Station OC receives sediment from both the Santa Monica Shelf and local cliffs. Cabrillo Beach receives sediment from the San Pedro Shelf and local cliffs. Station 8D plots in-between the effluent sample and White's Point Cliff, indicating fairly equal influences from both sources. Station 3A receives sediments from local and effluent sources.



The ratio of local to distantly derived quartz is shown in map form in figure (30). Highest ratios are off Portuguese Bend, where the slide is an abundant source of Altamira Shale. Higher values extend off the shelf to the west, due to the increasing importance of local material relative to effluent material in the farfield. Very low ratios near the outfall show the dominance of effluent input to the bottom in the nearfield. Closely spaced isograms are present between the two major sources--the slide and the outfall.

The distribution of these ratios in the pre-discharge era, (Fig. 31) as defined previously, shows a much simpler pattern. There is a strong influence of local sources in the nearshore, with higher amounts of clear quartz to the north and east--towards the distant sources of this species. Compared to present-day distributions: 1) the high values present off Portuguese Bend are absent, since movement had not yet begun; and 2) the intense gradients and shoreward bowing of gradient lines around the outfall area are absent, proving that the present-day pattern is a result of the dominance of effluent discharge in this area.

The change in sediment mineralogy from pre-discharge to the present can also be shown on the triangular graph (Fig. 27). In this figure, arrows point from pre-discharge values to present values. In the sediments closest to the outfall (high clear quartz) the direction of movement is towards effluent value. 8D also heads towards the effluent value and shows the greatest amplitude of change. Samples further from the outfall generally show an increase of amber quartz relative to chert, with stable amounts of clear quartz. This change is towards the PB slide value. Thus, the first group of samples mostly reflects influence of the effluent, and the second group of samples reflects the influence of the slide.

Other components also show interesting distributions. Mica is an interesting component to trace since its hydraulic behavior will be more similar to that of clay particles. During pre-discharge times (Fig. 32), the percent of mica increases offshore (like percent clay) and westward along the shelf. At the present time, percent mica is highest off of the ell-shaped outfall, and are being transported west southwest from that point (Fig. 33).

Analyses of heavy mineral distributions are interesting since these are usually more uniquely associated with a single source. However, since they usually comprise less than 5% of the total population, their percentages in my study are within the boundaries of error. A stricter analysis requires the separation of heavy and light minerals and separate point counts of this fraction. With these caveats, I present my data. These mostly show dispersal patterns of natural sediments, since effluent appears to contain very few heavy minerals, probably since they settle out more rapidly in processing before discharge.

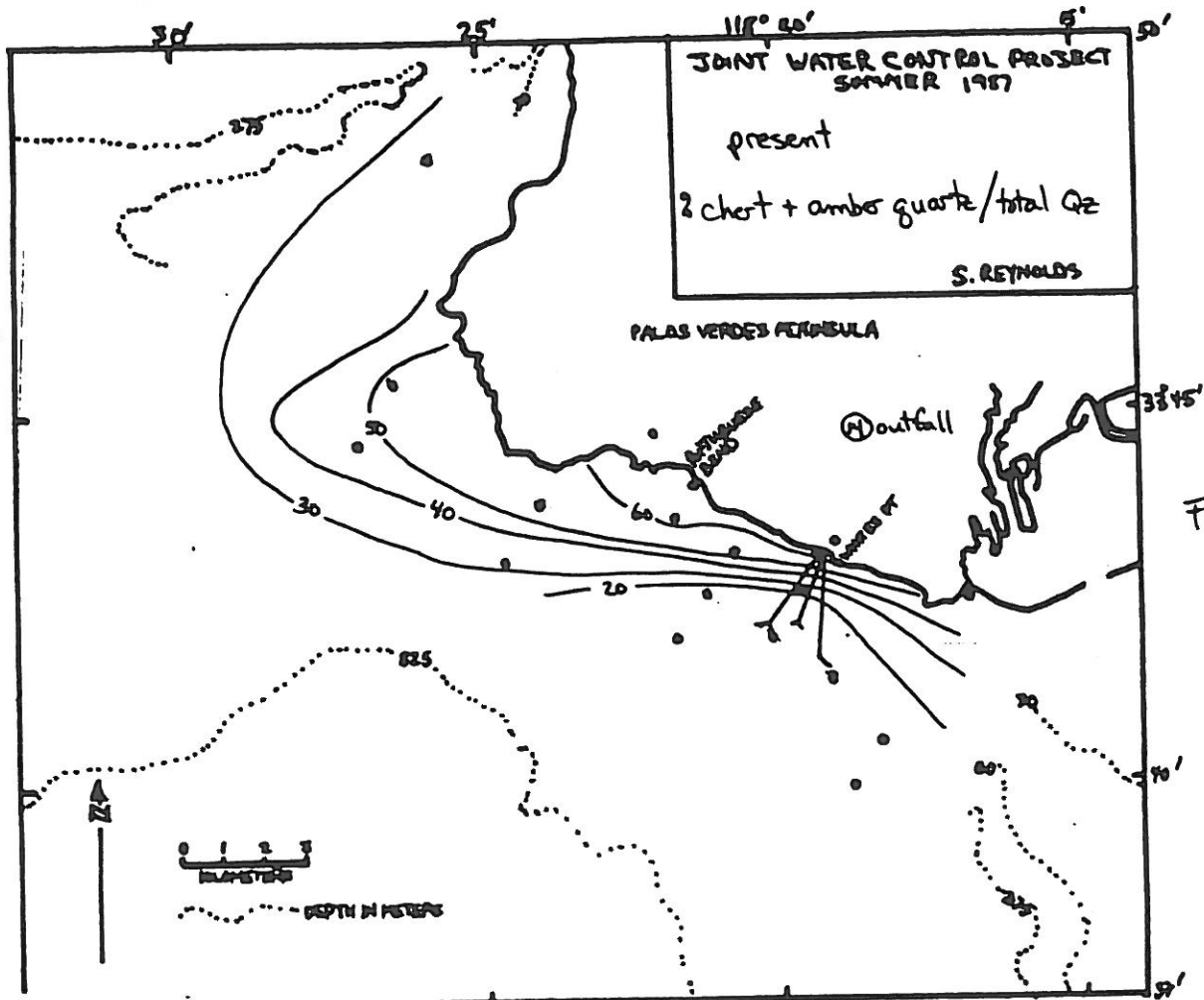


Figure 30

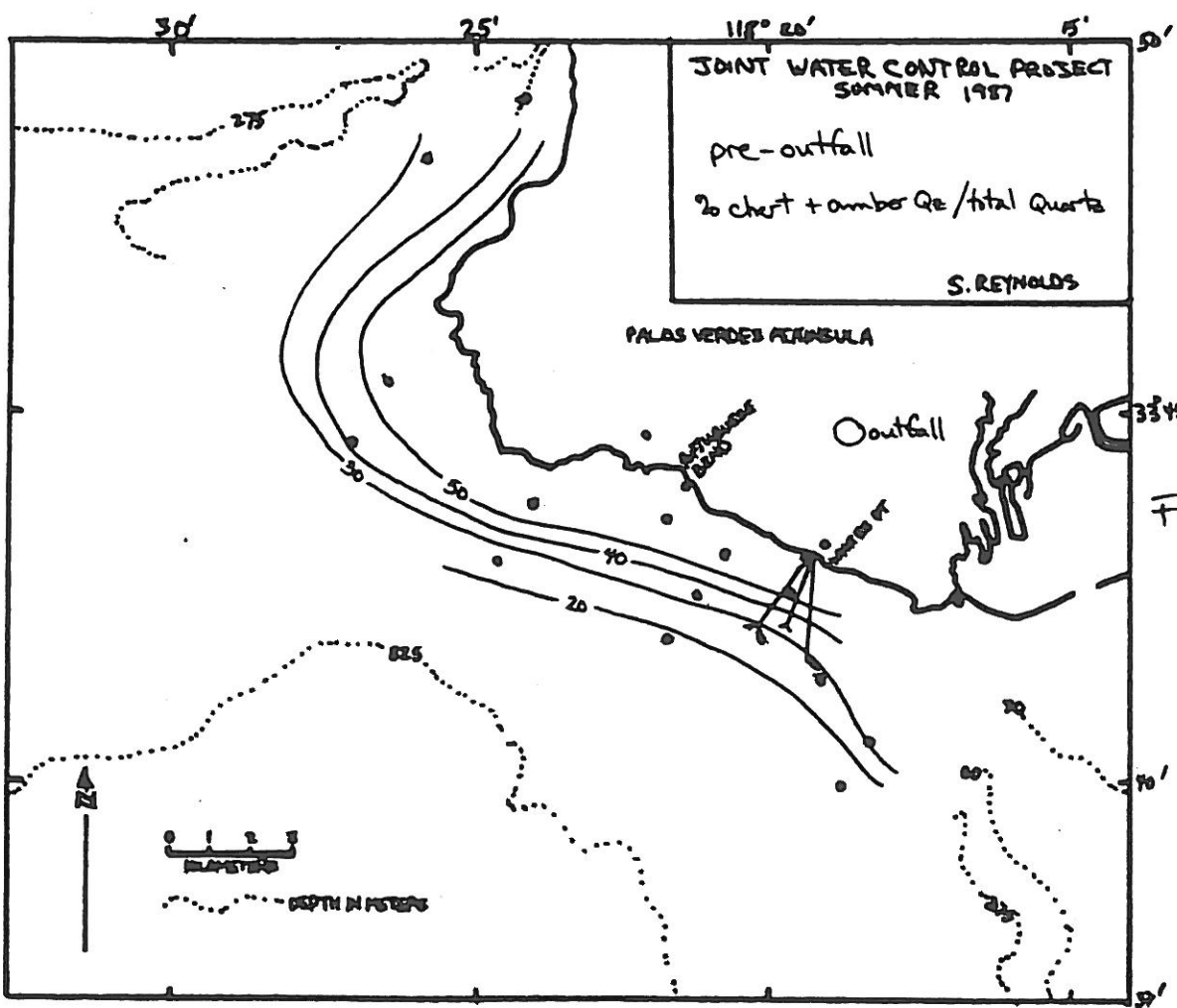


Figure 31

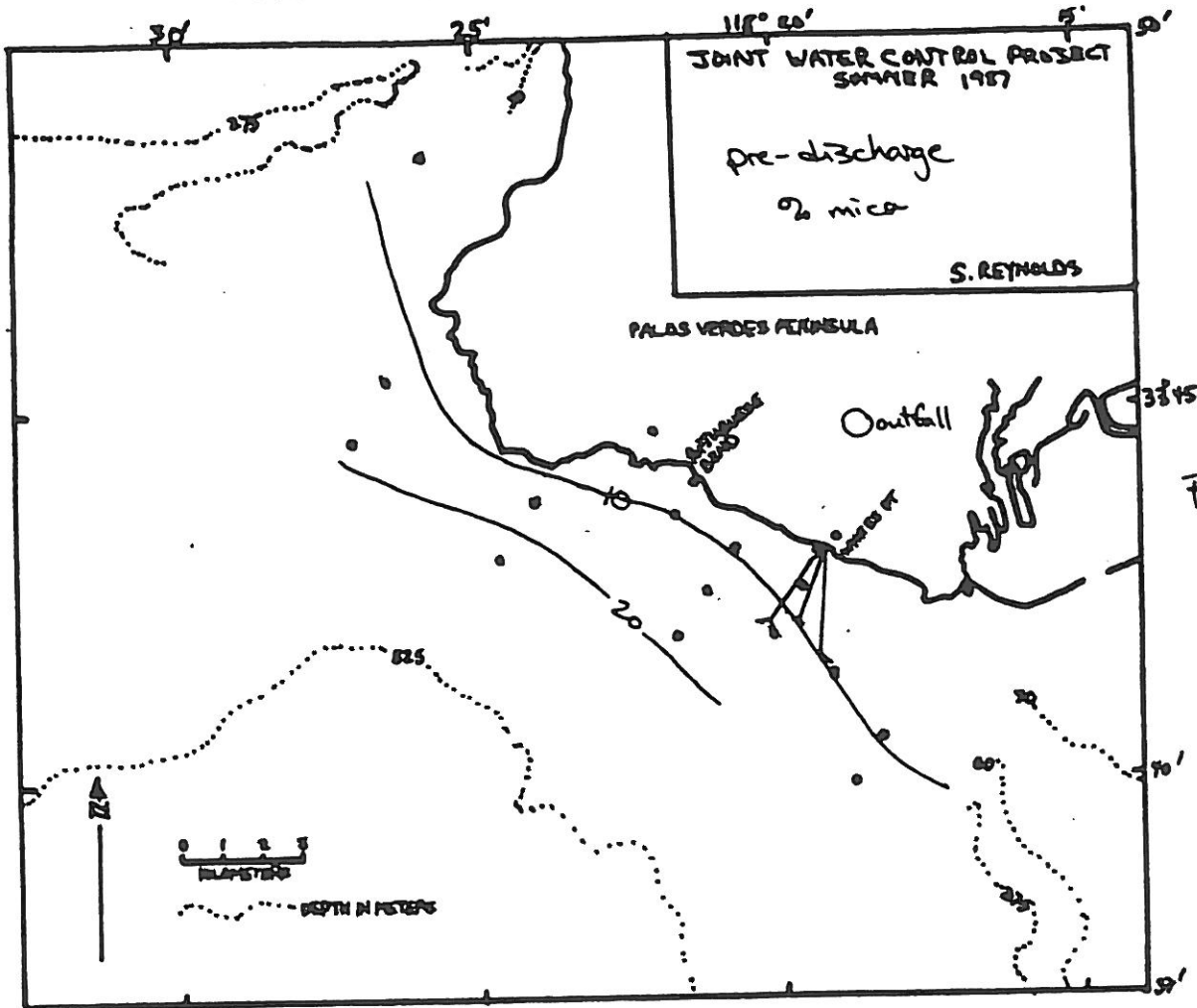


Figure 32

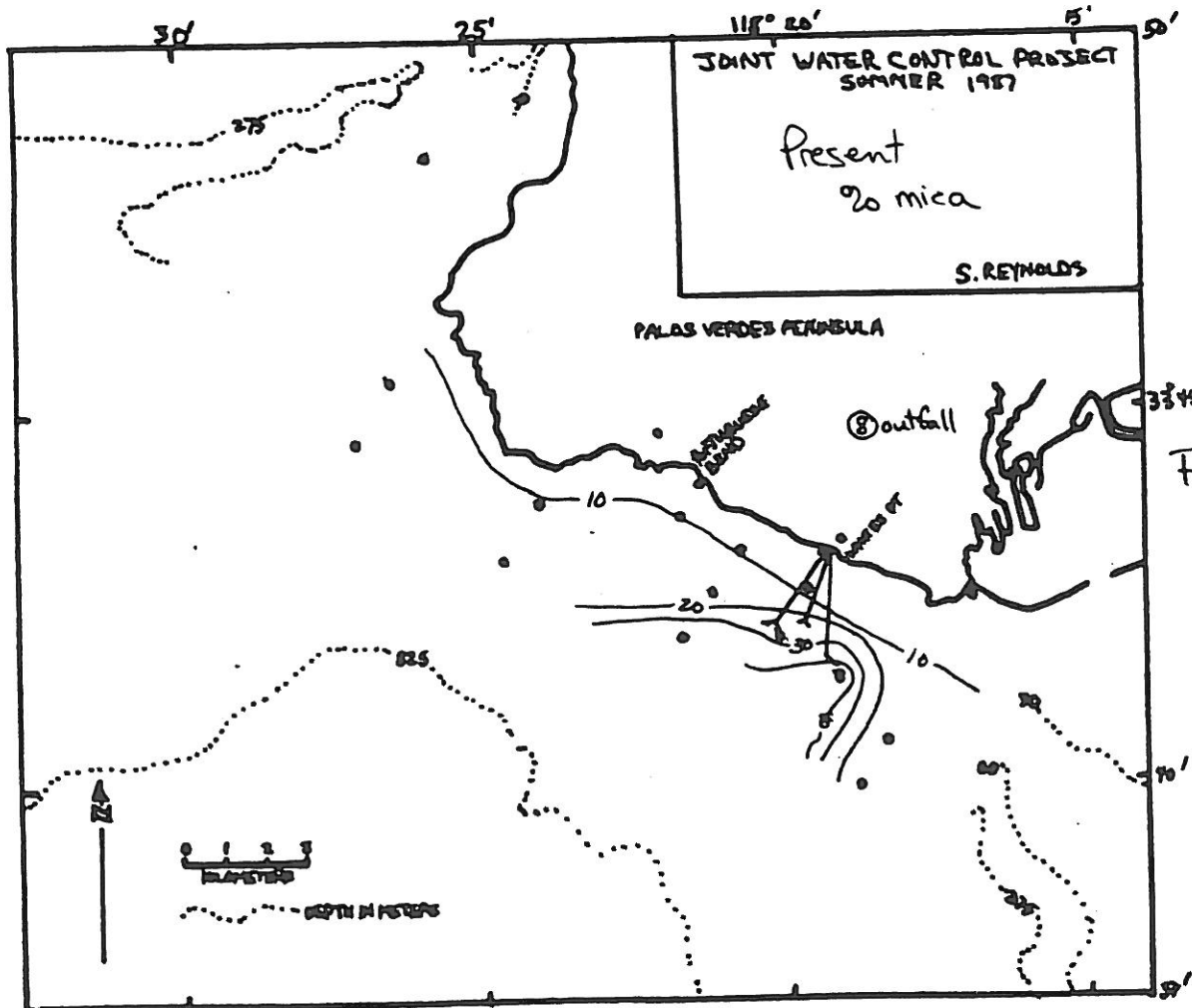


Figure 33

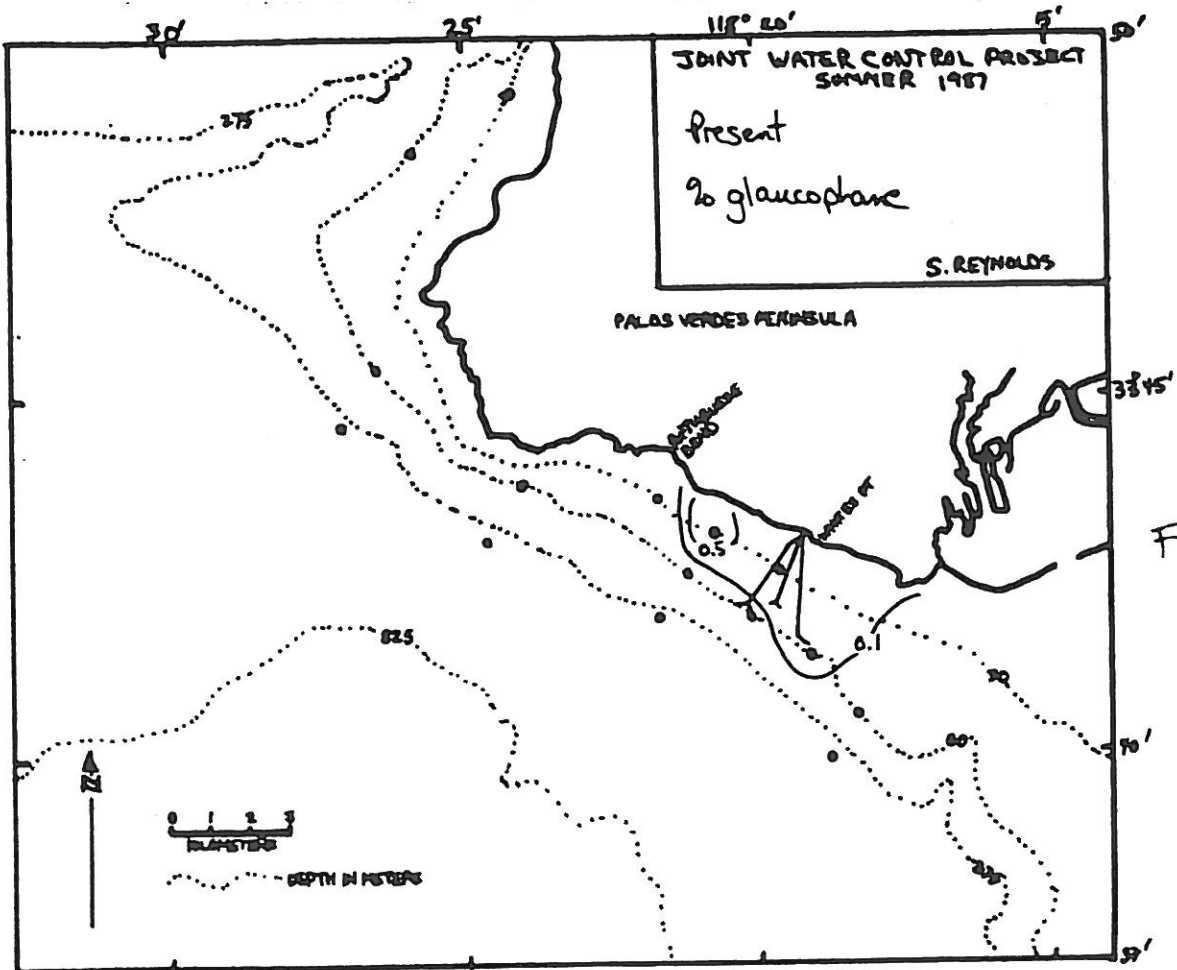


Figure 34

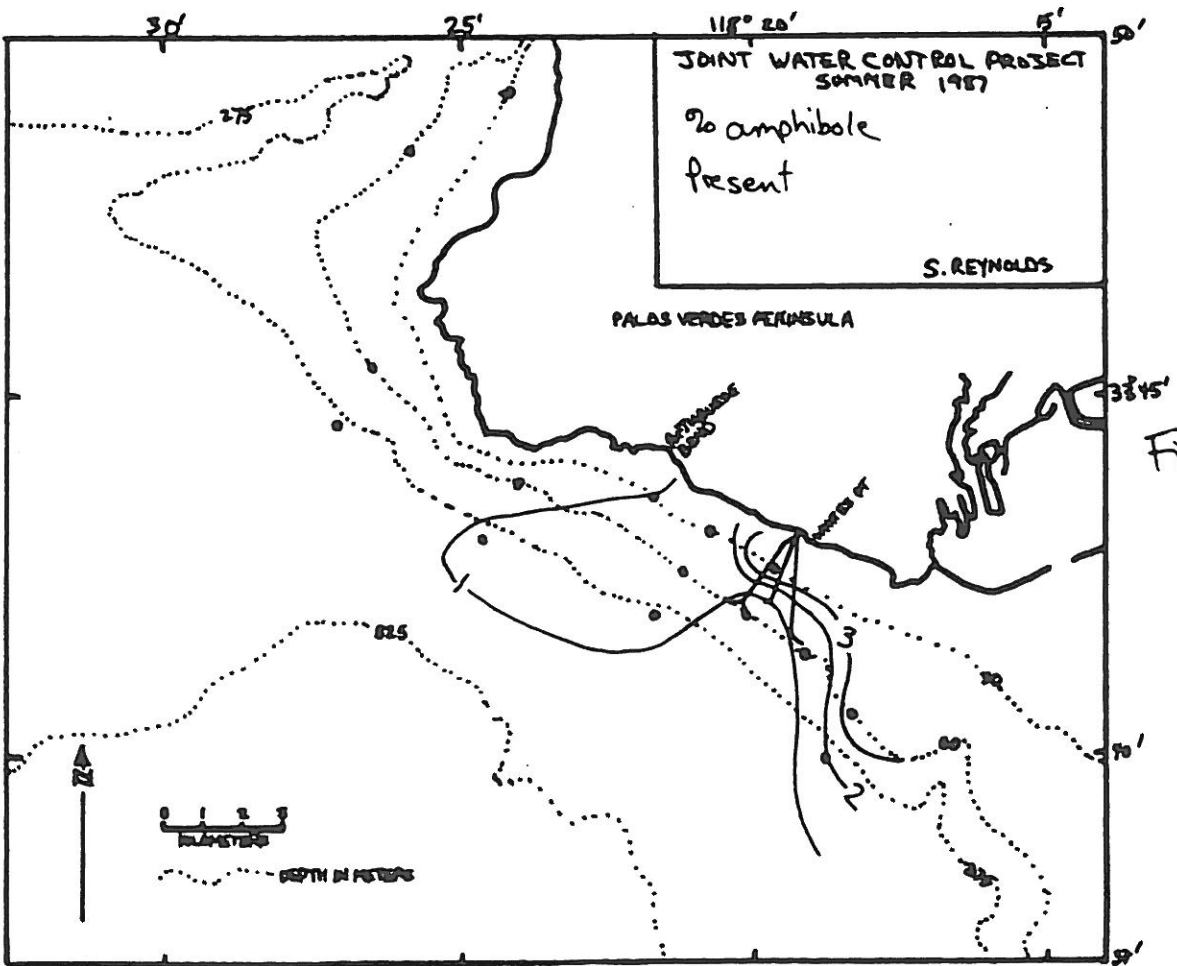
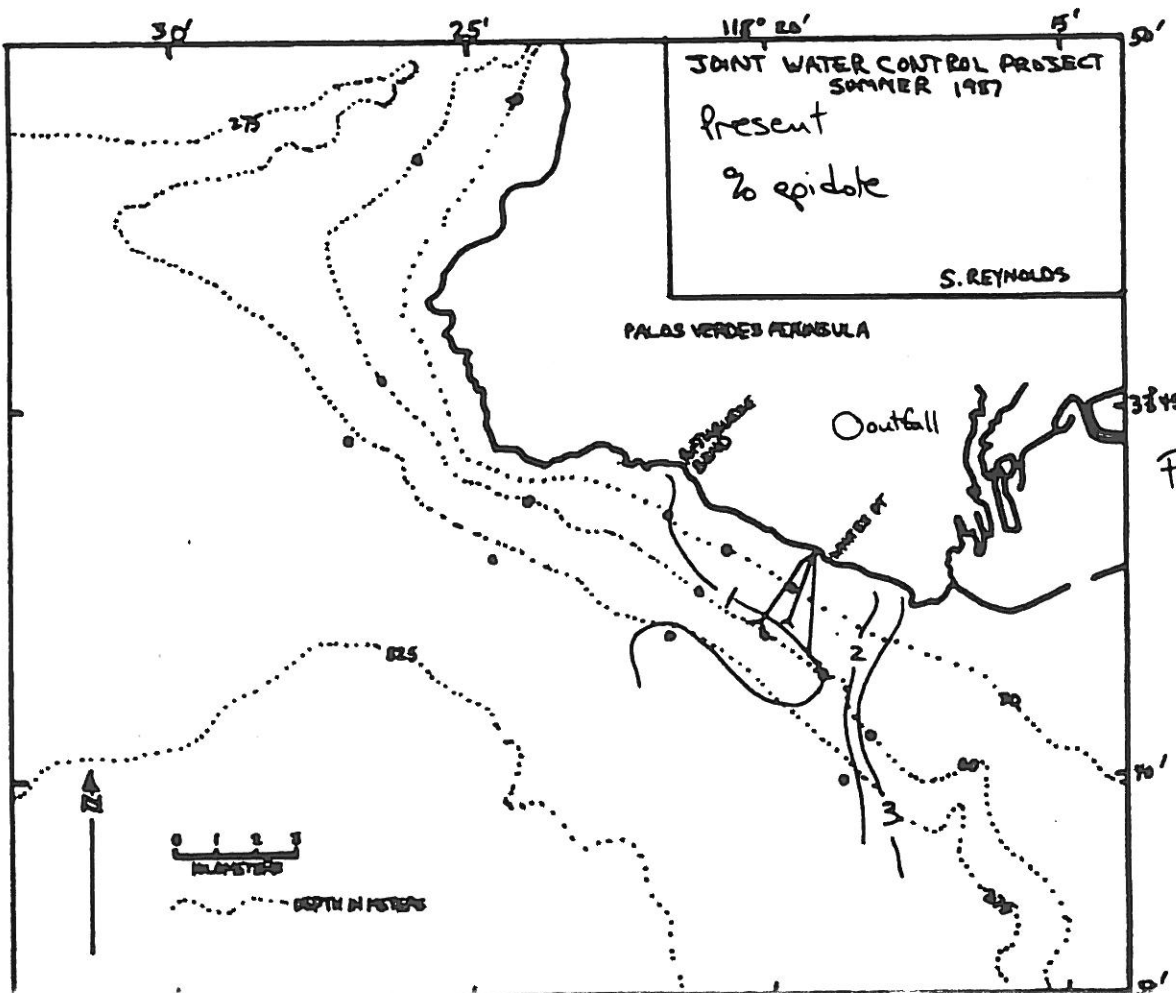
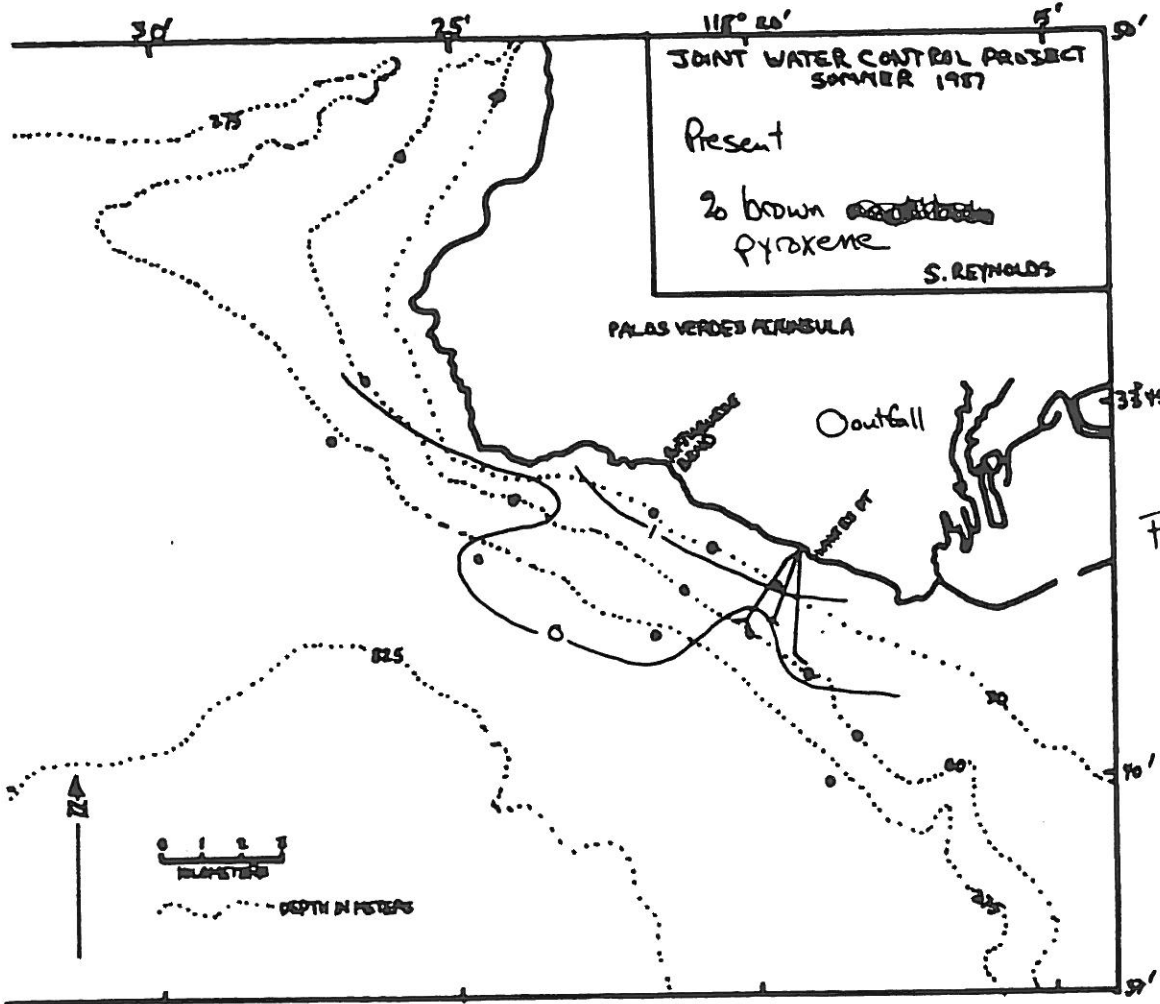


Figure 35



45

Glauconite and other blueschist minerals are derived solely from the blueschist arenite facies of the Altamira Shale. This forms part of the seacliffs from Point Fermin to White's Point, and crops out sporadically in the intertidal zone from there to Abalone Cove. In the marine sediments (Fig. 34), these minerals are found at stations 6D, 8D, and 9C, indicating that sediments from the seacliffs are reaching these areas.

Hornblende has two sources: the San Pedro Shelf and, to a lesser extent, the PV seacliffs. Percentages of this mineral (Fig. 35) are highest at Cabrillo Beach, and stations 10C, 10A, and 8D. These are derived from San Pedro Shelf. It is moderately high in stations 5D, 6D, 6C, 6A, and 3A. This illustrates offshore dispersal of sediments from the Portuguese Bend Slide.

Brown pyroxene is derived solely from Altamira Shale. A heavy-mineral concentration beach at the eastern end of Abalone Cove contains 20% brown pyroxene. In the marine sediments, (Fig. 36) percentages are highest in 5D, 6D, and 8D, showing input from seacliffs to these areas. This mineral is also present at stations 6C, 6A, 3A, and 9C, indicating offshore dispersal of seacliff and slide material.

Epidote is largely derived from the San Pedro Shelf, with Altamira Shale as a minor source. Concentrations are highest at station 10C (Fig. 37), and are generally higher towards the east and in the nearshore. Lower concentrations at stations 8C and 6C show the dilution effect of effluent input.

Percent organic material in the sand fraction has also changed dramatically through time. Prior to discharge (Fig. 38), no station had more than 1% organic components. During maximum effluent discharge (Fig. 39), however, 40% of the fine sand fraction in station 8C is organic in origin. This concentration drops off very rapidly within a few kilometers. Today (Fig. 40), organic material is only 5% of the fine sand at this station.

Several layers within cores 3C, 6C, and 8C have been interpreted as storm layers on the basis of grain size and x-radiograph stratification. These layers are relatively coarser than surrounding sediments; this coarsening could have been brought about through two methods: 1) storms could have winnowed out fine material, leaving behind in-situ coarser material; or 2) storms placed nearshore material in suspension, which diffused outward and settled offshore. In the first case, mineralogies of normal and storm sediments should be similar. In the second case, mineralogies of storm layers should be higher in amber quartz and chert, because these are more abundant in the nearshore compared to the offshore. When plotted on triangular diagrams (Figs. 41, 42, 43), these storm layers do plot closer to the amber quartz and chert axes, relative to normal depositional layers. Some exceptions do occur, probably as a result of the arbitrary 2-cm sampling interval. This supports the hypothesis that the fine sand in these storm layers at 60 m water depth are at least partly depositional, rather than erosional, in origin.

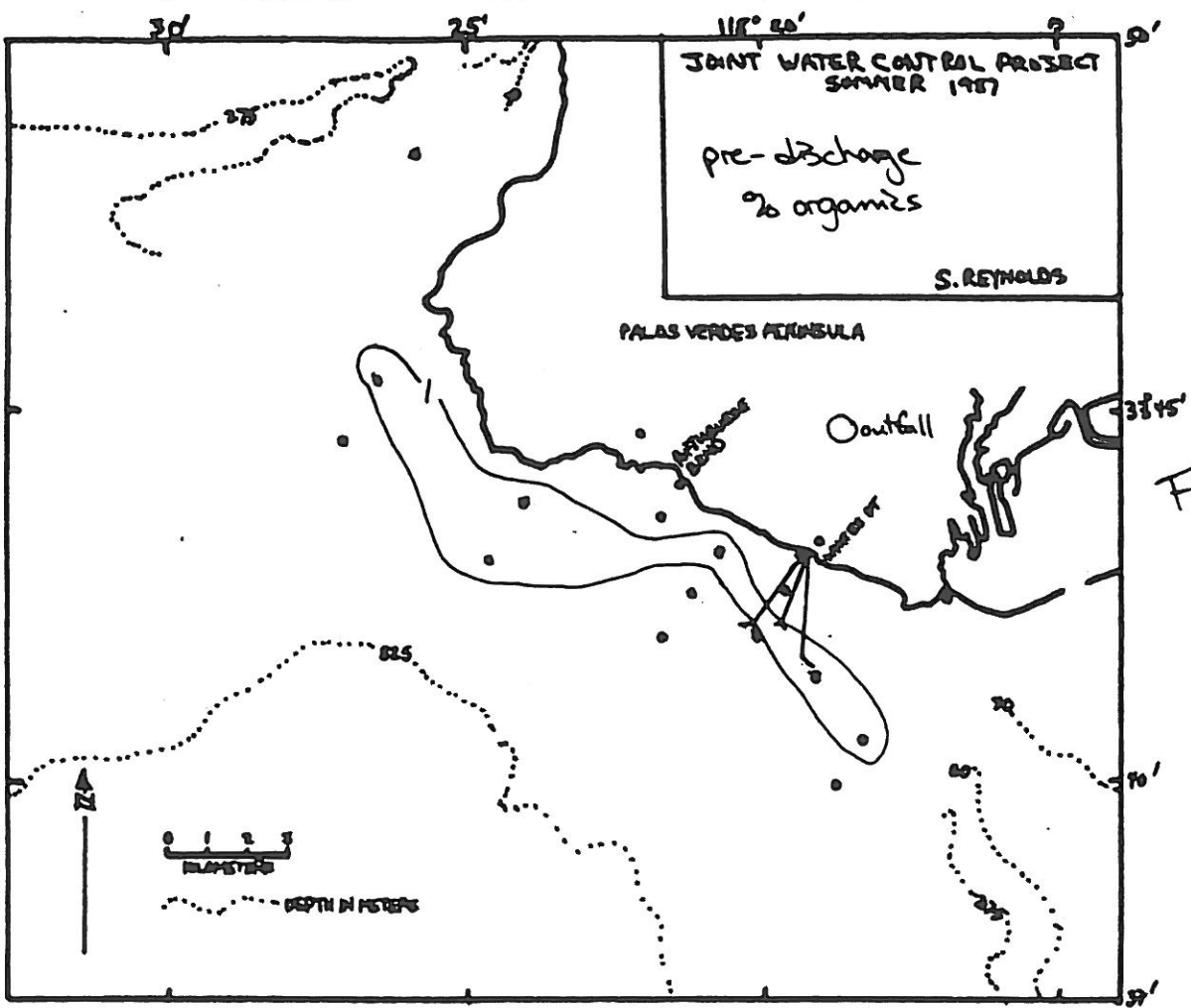


Figure 38

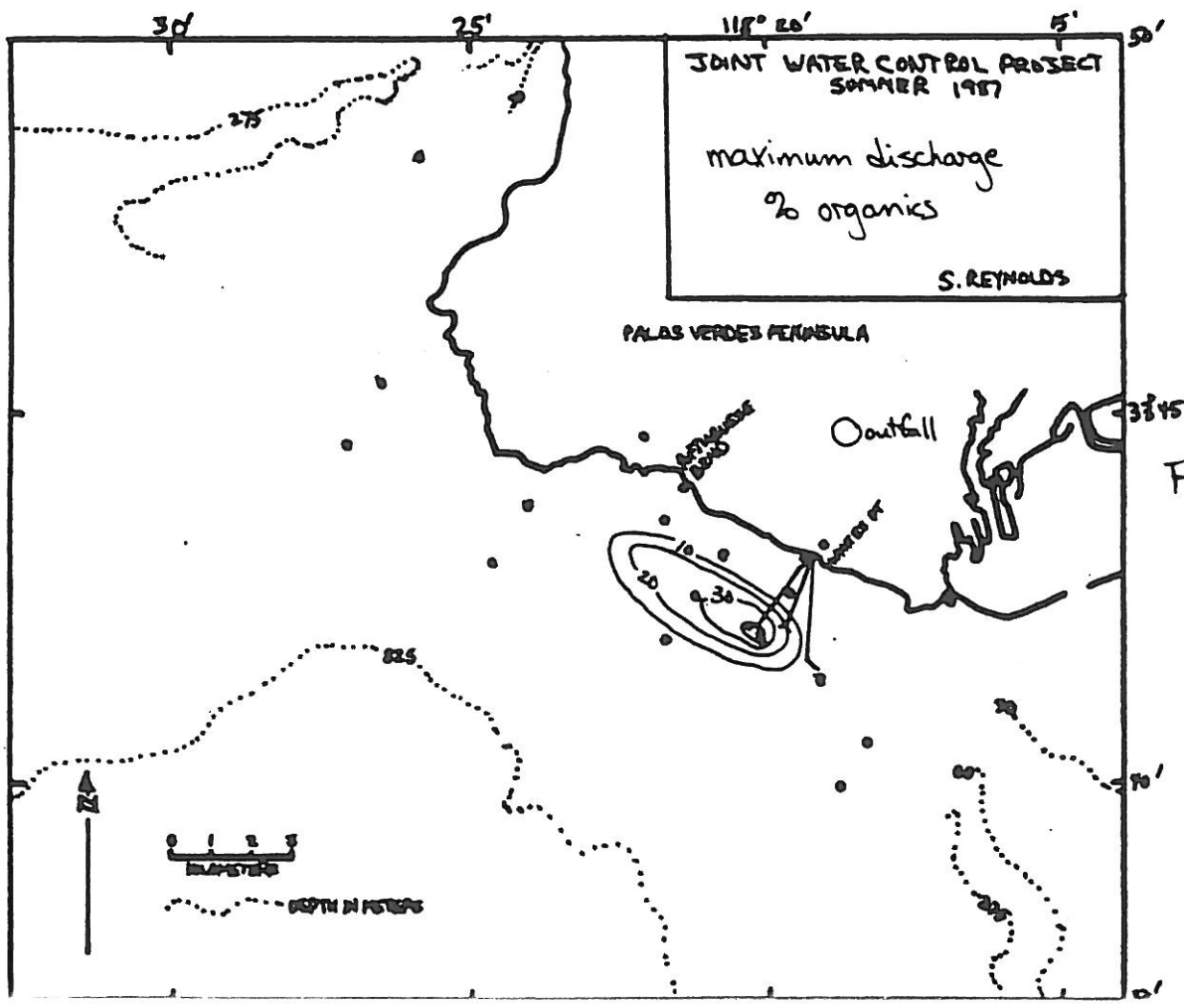


Figure 39

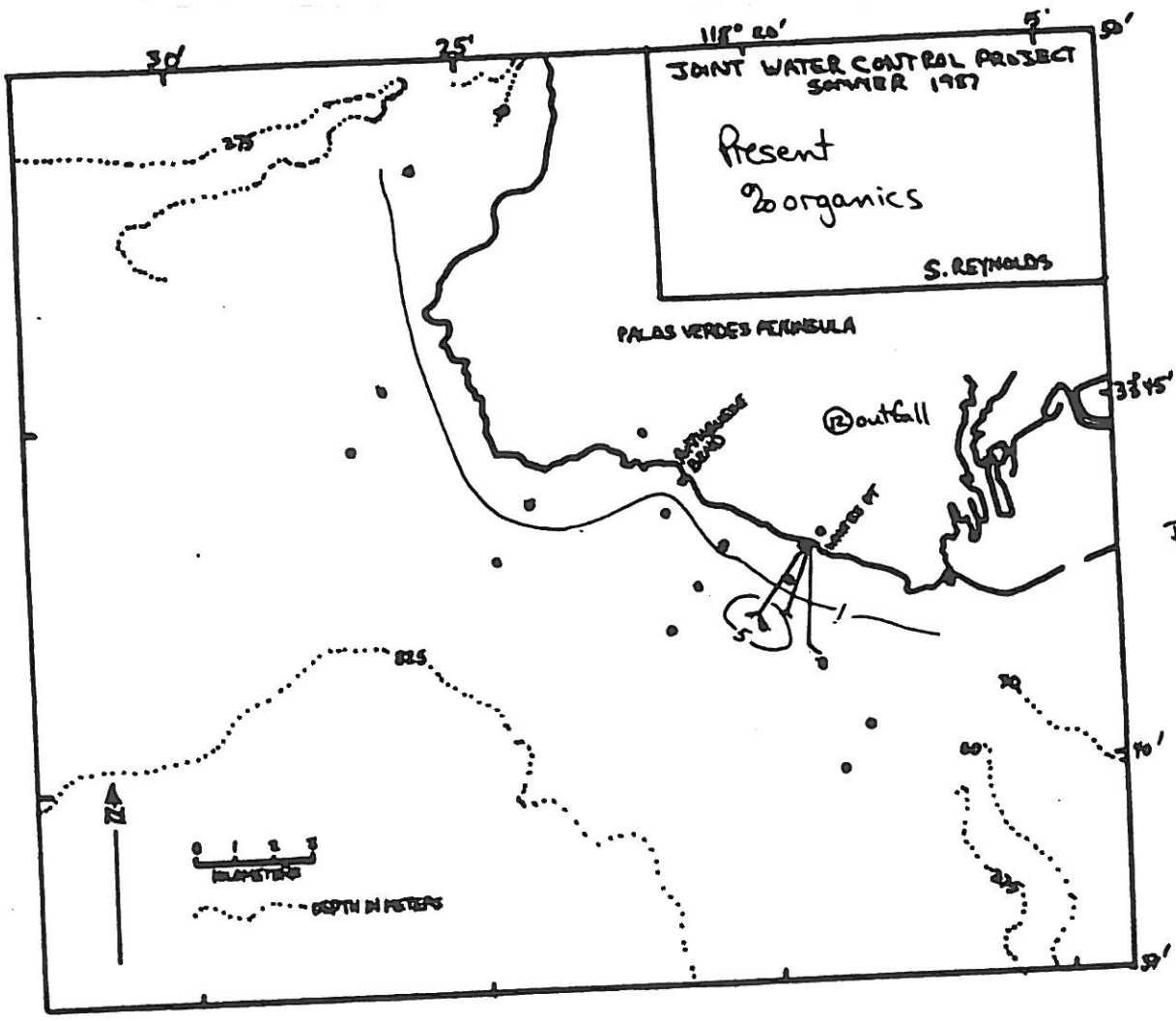


Figure 40

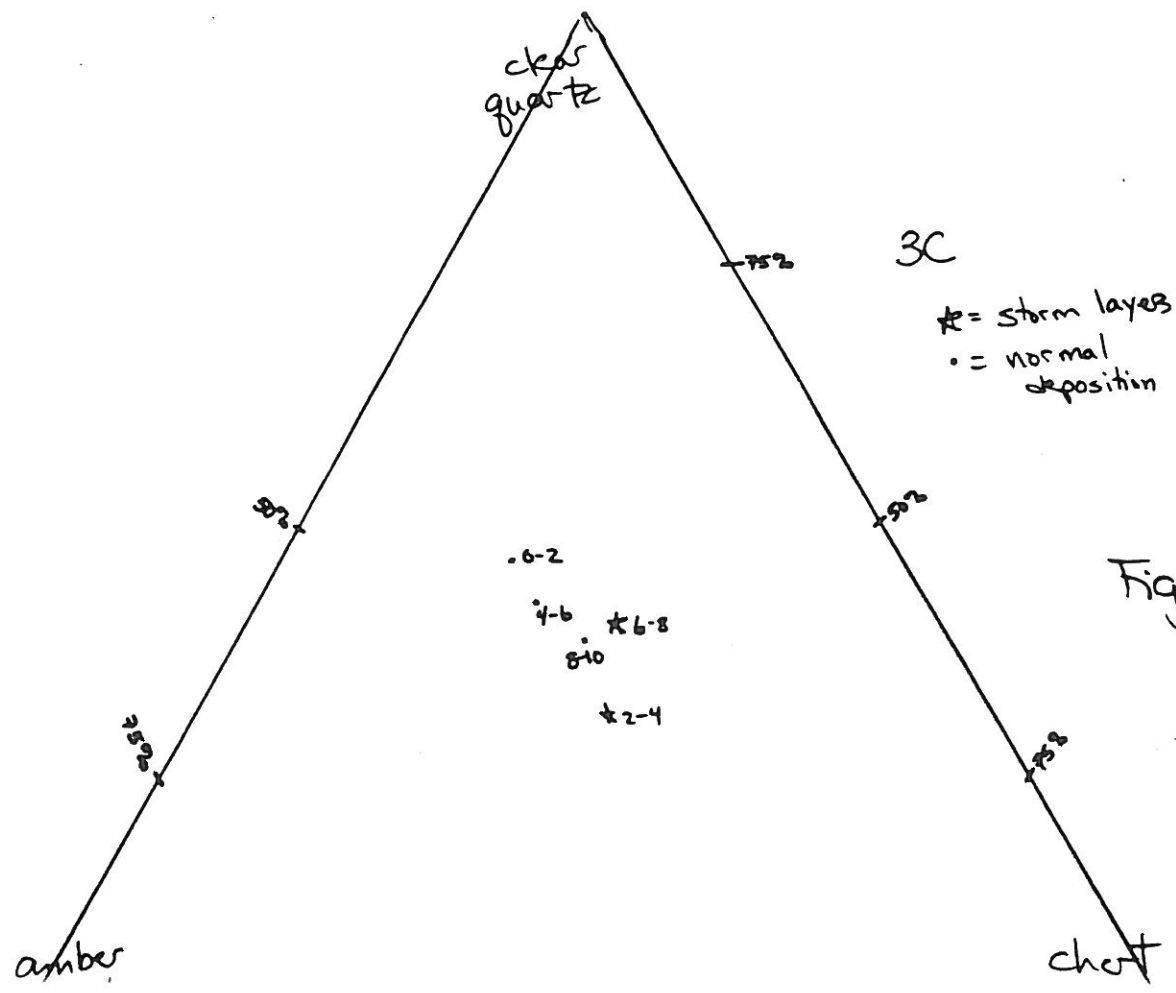
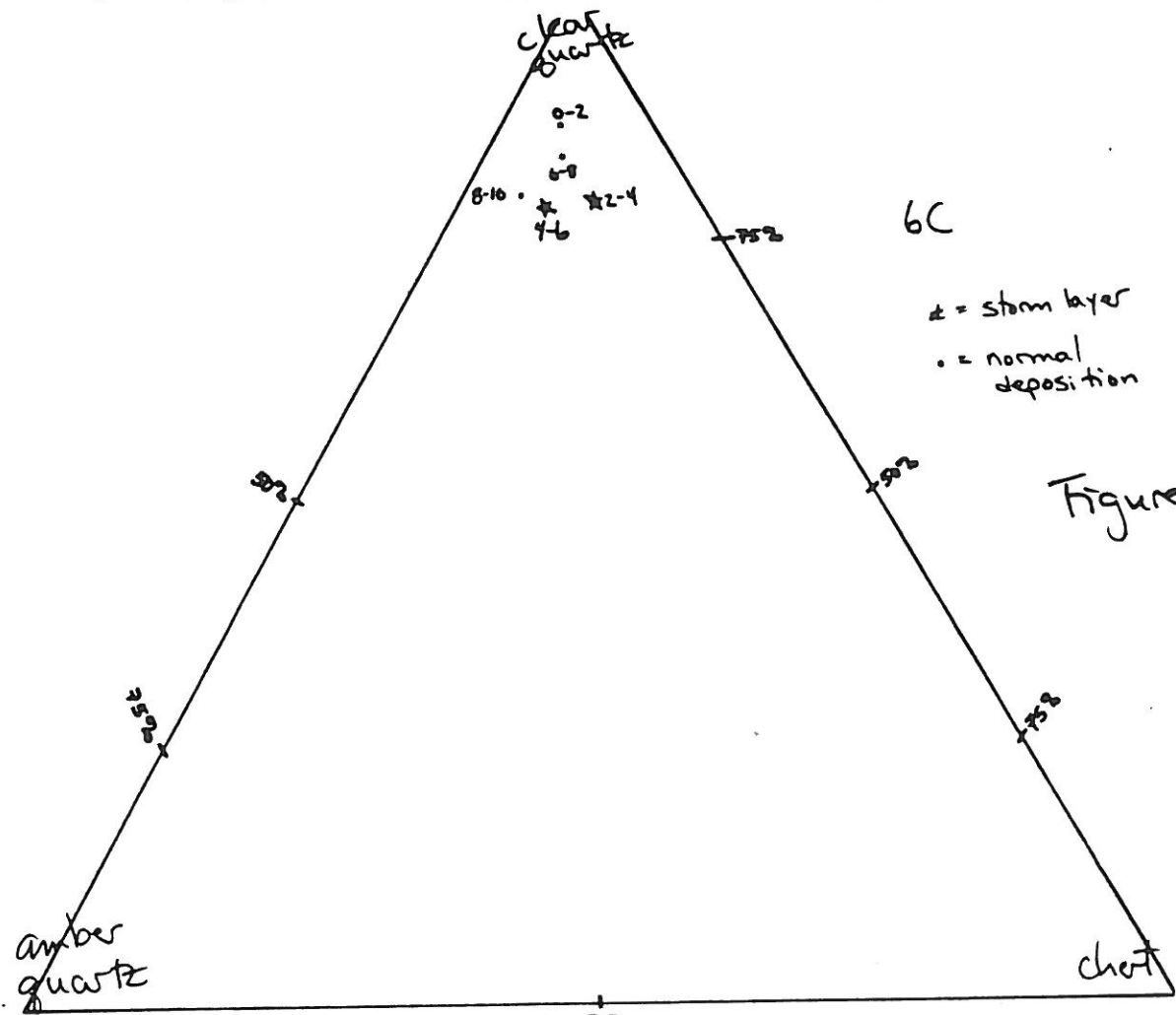


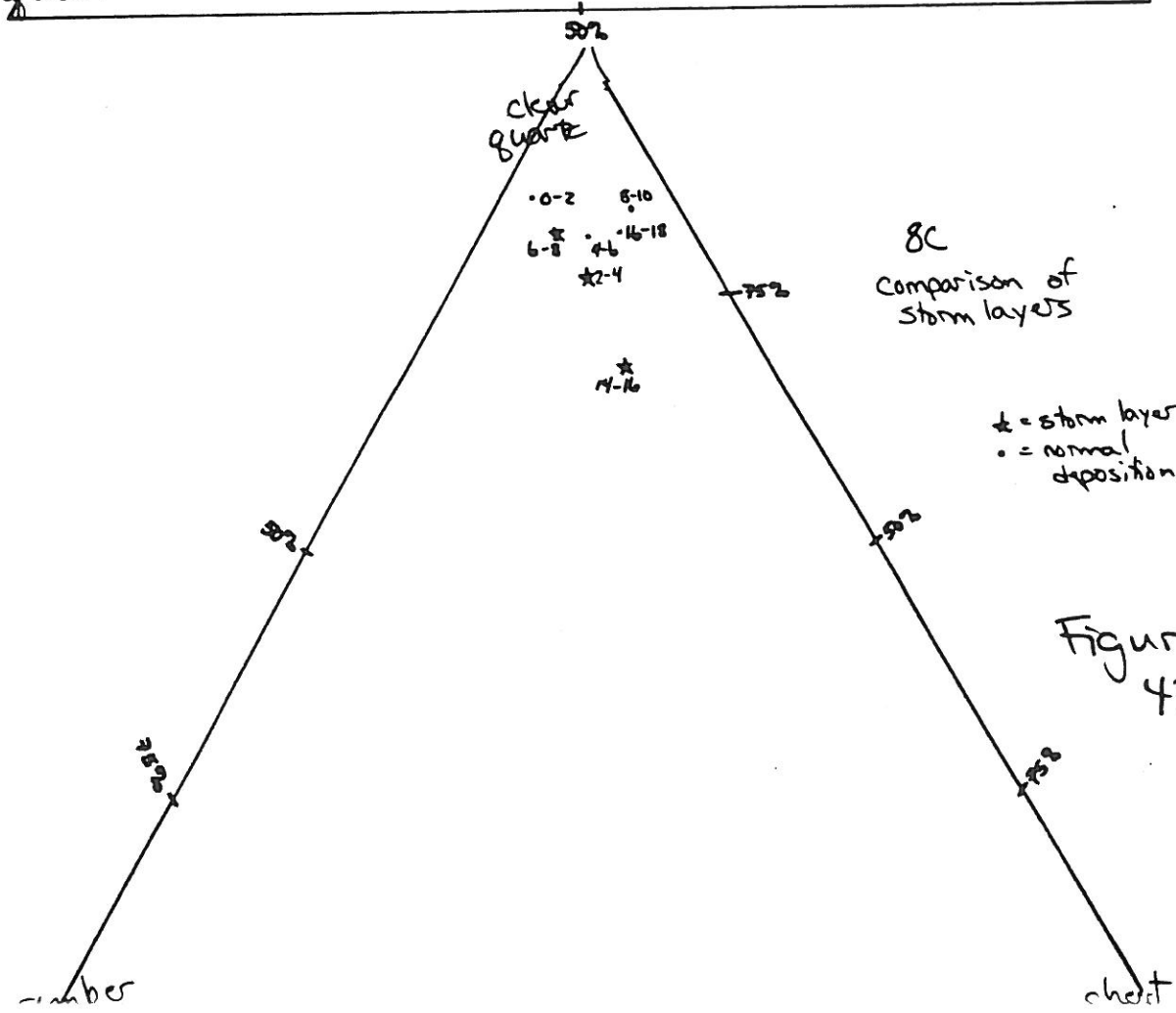
Figure 41



6C

* = storm layer
 • = normal deposition

Figure 42



8C
 Comparison of storm layers

* = storm layer
 • = normal deposition

Figure 43

MASS BALANCES

The fate of effluent particulates is essentially a mass balance problem. If we know how much material has been discharged onto the shelf, and how much remains, then we know how much has been lost by degradation and/or transport to deeper waters. I preface the following mass balance discussion by emphasizing that these numbers are only order-of-magnitude estimates. In addition, it is important to keep in mind the distinction between rates of sediment input and rates of sedimentation, the first term referring to the amount of material available for deposition, and the second term referring to material which is actually deposited.

Rate of input: effluent

My estimates of solid discharge from the outfall are:

- since 1937: 3.8×10^{12} g
- since 1956: 3.3×10^{12} g

These numbers expressed as rates are:

- 1956 to 1970: 11.5×10^{10} g/yr
- 1970 to 1985: 11.0×10^{10} g/yr
- 1987: 4.0×10^{10} g/yr

Rate of Input: PB slide

Approximately 7.5×10^6 yd³ of material has been eroded from the toe of the Portuguese Bend slide since 1956 (Ehlig). Given that 1 yd³ = 1.5 tons, and that approximately 1/3 of this material remains on the beach (Ehlig) this provides:

$$6.7 \times 10^{12} \text{ g since 1956}$$

This number expressed as a rate is:

$$22 \times 10^{10} \text{ g/yr}$$

Rate of Input: Seacliff Erosion

Seacliff erosion is an episodic, non-uniform process, so it is difficult to give an exact value except by studying aerial photographs of the shoreline through time. However, a rough estimate for the amount of seacliff retreat in Palos Verdes is about 2" per year, ranging from 9" to 0.2" depending on the lithology of the cliff material (Griggs & Savoy, 1985). Using:

30.5 m = average cliff height

1.6 m = retreat since 1956

15 km = length of coast from Pt Fermin to PV Point

This provides an estimate of:

1.4×10^{12} g since 1956

Expressed as a rate, this number is:

4.7×10^{10} g/yr

Rate of Input: Denudation

Denudation of the Palos Verdes Peninsula is caused by stream erosion and is measured by an average lowering of the land surface. No direct measurements of denudation have been made for PV, but empirical relationships which have been derived from data in other areas (Taylor, 1981) can give us an idea of the magnitude of this material. Taylor's equations yield a denudation rate of 0.5 mm/yr; the area of the western half of PV Peninsula is 42 km²; and assuming density of surficial sediments to be 2 g/cm³, yields:

1.3×10^{12} g since 1956

Expressed as a rate, this is:

4.2×10^{10} g/yr

Rate of Input: Totals

Total input from natural sources is:

9.4×10^{12} g since 1956

Total of all input is:

12.7×10^{12} g since 1956

The Post-1956 Deposit

The characteristics of this deposit are as follows:

| | |
|-------------------|------------------------------|
| Area: | $6 \times 10^7 \text{ m}^2$ |
| Total Volume: | $6 \times 10^6 \text{ m}^3$ |
| Weight of solids: | $3 \times 10^{12} \text{ g}$ |

This represents only about 25% of all material available for deposition on the shelf. The rest of the material could have been lost by:

- 1) non-deposition of clays derived from natural sources. The PB slide and the seacliffs are composed of Altamira Shale, which is dominantly clay. This material is input into the marine system at the shoreline, mostly during storms--thus only at times and places which would be least likely to induce clay sedimentation.
- 2) non-deposition of clays from the effluent. Less likely to occur since this material is input into the marine environment continuously, at deeper, quieter waters more conducive to clay deposition. In addition, the presence of large amounts of organic material increases clay flocculation and thus settling velocity.
- 3) degradation of organic material in effluent. Myers states that 70% of the effluent solids are organic material; after a few weeks to a month on the shelf, this value decreases to 42-58%. This suggests that 12-28% of effluent solids are lost to the degradation of organics, leaving 72-88% of this material available for long-term deposition.
- 4) very nearshore deposition of PB slide. Sand mineralogy of surface sediments do not show that this material is significantly input into the marine system more than a few km away from Portuguese Bend. The fining-upwards storm deposits at station 5D certainly represent at least a large part of this material. To examine this possibility, let us consider the storm of 1983, during which $3.8 \times 10^5 \text{ m}^3$ was eroded from the toe of the slide. A rough estimate of the potential area of this deposit is 6 km^2 ; extending from 3D to 6D, but not into C stations. This yields an average thickness of 6.3 cm if all of that material was deposited in the nearshore area. The 1983(?) storm layer at station 5D is 18 cm thick. Considering the total supply of slide material since 1956, yields a deposit which would average 1 m thick. This is not unreasonable.
- 5) Winnowing of clay and silt during storms. This probably occurs to some extent, as shown by downcore grain size distributions.

SEDIMENTATION RATES

The following numbers are rates of sediment supply per the area of the post-1956 deposit, and are not sedimentation rates. I include them merely for comparison with actual sedimentation rates.

PB slide: 370 mg/cm²/yr
 denudation: 70 mg/cm²/yr
 cliff erosion: 70 mg/cm²/yr

 total natural: 510 mg/cm²/yr

 effluent: 161 mg/cm²/yr

 effluent 1987: 66 mg/cm²/yr

Estimates of actual sedimentation rates were determined from downcore data for each station. These numbers are now accumulation rates rather than supply rates.

| <u>Station</u> | <u>mg/cm²/yr</u> | <u>cm/yr</u> |
|----------------|-----------------------------|--------------|
| 1A | 20 | 0.12 |
| 3A | 40 | 0.22 |
| 6A | 80 | 0.48 |
| 10A | 20 | 0.12 |
| 1C | 70 | 0.45 |
| 3C | 170 | 0.87 |
| 6C | 260 | 1.38 |
| 9C | 80 | 0.45 |

The first point to make is that the natural sedimentation rate cannot be greater than 20 mg/cm²/yr, but may be close to this number. Probably 10-15 mg/cm²/yr is the best estimate. This means that 97-99% of the sediment naturally supplied from Palos Verdes Peninsula either remains very nearshore or is transported off the shelf (west, east, or offshore). Working backwards, this also means that 78-84% of the solid material discharged from the outfall remains on the shelf. The loss of this material can be explained by degradation with very little room for loss due to transport.

Today's Sedimentation Rates

Natural: 20 mg/cm²/yr

Effluent average: 66 mg/cm²/yr

| | | | |
|-------------|----|----|----|
| by station: | 3A | -- | 8 |
| | 6A | -- | 25 |
| | 1C | -- | 20 |
| | 3C | -- | 61 |
| | 6C | -- | 98 |
| | 9C | -- | 33 |

SEDIMENT DYNAMICS ON THE PV SHELF

FAIR WEATHER

Effluent discharges at 60 m water depth; since this is fresh-water entering salt-water, a bouyant plume rises above the seafloor. The local current regime moves this plume towards the west before the particles settle out. Virtually all of this material is rapidly flocculated by organic material and is deposited within several km of the outfall. Perhaps 10-20% of this material degrades very rapidly.

Small to moderate waves breaking against the Portuguese Bend slide continuously erode it. Clay-sized material travels eastsoutheast in suspension in the surface nearshore waters. Apparently the salinity boundary between outfall water and nearshore water inhibits the movement of this material over the outfall area. This material may be temporarily deposited in the nearshore.

Longshore drift carries very nearshore sand towards the east. Surface waves may cause minor movement of sand and silt onshore or offshore. Bottom currents, moving towards the west, may cause minor movement of sediments towards the west.

LOCAL STORMS

High amounts of rainfall create ephemeral streams and sheet runoff which erodes surficial material from the peninsula, carries it down canyons into the nearshore marine environment. Depending on the energy conditions at the coastline, the coarsest of these particles will be deposited on the beach, and progressively finer and finer particles will be deposited offshore. Clay material will probably be carried in suspension off the shelf. Sand and silt from this source may be deposited on the shelf.

High-energy waves breaking against the shoreline will erode seacliffs and the Portuguese Bend. This is not a uniform process in space and time. Waves break against the base of the cliff and undercut it, leading to instability and collapse of the upper part of the cliff onto the beach, where continued wave activity will eventually disaggregate these rocks into particles which can be deposited further offshore. How far offshore is the salient question. In the case of slide material, it appears that much of the coarse material remains in the nearshore. However, much of the clay may be carried off the shelf. Small amounts of sand, silt, and clay derived from the PB slide are deposited on the shelf directly seaward and westward of Portuguese Bend.

BOTTOM STORMS

The water depth at which waves affect the seafloor is dependant not on wave height, but on wave length. This depth is generally taken as $1/4$ to $1/2$ the wavelength. Local storms form waves which have high height and energy, but fairly short wavelengths. Waves with the longest wavelength are formed from equatorial hurricanes, which travel north into the Southern California Bight. These are the waves which may cause "bottom storms" which would be responsible for much of the resuspension of shelf material at greater than 50 m water depth. So, local storms create deposition on the central and outer shelf, and distant storms create the erosion in this area.

During these "bottom storms," resuspension probably involves less than the upper cm of bottom sediment. The finer silt and clay particles will preferentially be put into suspension. The local current regime, if operative, will move them downstream to the west. Otherwise, this fine material may remain in suspension and diffuse outwards. Probably most of the silt is redeposited fairly close to where it originally came from. Sand is probably not resuspended.

Another potential energy source for bottom storms is the deep slope current measured by Barbara Hickey, which reaches velocities up to 1 knot. We do not know if this current impinges upon the bottom, or what that bottom velocity would be. A final possible agent for resuspension of deep sediments is breaking internal waves.

POSSIBILITIES FOR THE EXHUMATION OF THE BURIED DDT LAYER

EROSION

At the present rate of deposition, and probably even at reduced rates of effluent discharge, it is not likely that the DDT layer will be exhumed by erosion at stations 8C, 6C, and 3C. Current rates of deposition, 3 to 5 times the natural rate, result in accumulation of about 1 cm per year; at this water depth, resuspension of greater than the upper cm of sediment is unlikely during any single event.

DDT is also buried in sediments at station 8D. It is not known whether DDT is present at depth in other stations at 30 m water depth. It is possible that some local erosion has already occurred at 8D, but whether this erosion occurred during pipeline construction and maintenance, or whether it occurred through natural causes is not known. In any case, events occurring at station 8D cannot be extrapolated to other nearshore stations because 8D, located between the pipelines, will have distinctly different sediment dynamics. Erosion at this water depth is possible, but we have no data to support this possibility, and also no data to show that large quantities of DDT would be exhumed if this erosion occurred. Monitoring of other 30-m stations should be initiated, particularly 7D.

If, in the future, exhumation of DDT at this water depth was determined to be occurring, the solution to this problem would not be as simple as adjusting the amount of suspended solids contained in the effluent discharge. The material in the effluent is fine-grained; fine-grained material does not, in general, move towards the shoreline, but away from it. Locally, it does appear that a significant amount of effluent material is deposited between the pipelines, but we do not know if natural processes brought this material here, or if it is coming from leaks in the pipeline. Very little, if any, effluent material reaches stations 6D and 5D. If coarser (mineral) material was discharged, there would probably not be enough energy at 60 m water depth to move it back onshore. So the solution would be a difficult problem.

Erosion on the outer shelf and slope samples could be caused by strong slope currents measured by Barbara Hickey. It is important to know if these currents impinge on the seafloor, and what their bottom velocity is. DDT profiles at station 6A should be monitored closely.

The northwestern edge of the deposit (1C, 1A) is another area of concern. Sedimentation rates are low, and the DDT peak is close to the surface. However, we have no evidence that erosion here has occurred in the past. Resuspension of bottom sediments at these water depths appears to involve less than the upper cm of sediment, and the DDT peak is buried at 5-10 cm subbottom depth, so exhumation of the DDT is possible, but not probable at the current rate of deposition.

The eastern edge of the deposit (10C, 9C, 10A) is also an area of concern. This area receives less sediment from effluent discharge since prevailing bottom currents are towards the west. It does receive sediment from the San Pedro shelf, but much of this sediment travelling westward will be trapped within the San Pedro Sea valley. Sediments from the San Pedro shelf probably travel westward in the nearshore, and are moved offshore from around station 10D during storms. In addition to the relatively low rates of sediment supply to this area, there is also a strong likelihood of greater current activity in this area. Submarine canyons alter current and wave regimes on the nearby shelf, and oftentimes are characterized by fairly strong currents. At least one small area in the vicinity of station 10C has a hard substrate, and grain sizes and mineralogies of the surface sediments at both 10C and 10A suggest the possibility that these are winnowed deposits. At present, there is no data proving that erosion has occurred in this area, but continued intensive monitoring and study is needed.

MASS MOVEMENT

Characteristics of a marine environment which makes it prone to mass failure are: high sedimentation rates, steep slopes (>1), an abundance of silt, and the presence of high-energy triggers (wave pounding, earthquakes). Most of the southern Palos Verdes Shelf meets these criteria abundantly. There is no evidence in the cores that mass movement has occurred, with the possible exception of station 8C. This station should be studied carefully.

Other than general characteristics of the environment, we have no data to evaluate the likelihood of mass movement. Geotechnical testing of the sediments to determine their strength would be relatively easy to perform. I would caution that a box core, rather than the SCCWRP corer, would be better for collecting sediments for this type of testing. Care should be taken to minimize disturbance of the sediments, and to test them in as realistic and quantitative manner as possible.

In order to find out if mass movement has already occurred, geophysical profiling is a more efficient method than coring. This should include both high-resolution subbottom profiling and side-scan radar.

Continued dumping of sewage will lead to increased instability of these sediments. Thus this problem will become of increasing importance as the years pass and the possibility of mass failure should be evaluated now. In addition, I should point out that the SCCWRP suggestion of capping the deposit with 10 cm of sand would cause catastrophic results. These sediments are soupy, and dumping dense material on top would lead--at the minimum--to stirring, and at the maximum, to catastrophic mass

failure involving the entire sediment pile and wholesale exhumation of the buried DDT.

BIOTURBATION

Bioturbation is probably a very effective method of exhuming the buried DDT layer, particularly if decreasing amounts of effluent discharge leads to the establishment of larger populations of more deeply-burrowing organisms in the outfall area, where the highest amount of contaminants lie buried.

My data do not say much about bioturbation. All sediments have been thoroughly bioturbated, but the depth of mixing is not known. More study should be done to learn the life habits of these organisms.

REFERENCES CITED

Grigg, G., and Savoy, L. (1985) Living with the California Coast, Duke University Press, North Carolina, 393p.

Taylor, B.D. (1981) Sediment management for Southern California mountains, coastal plains, and shoreline, part B: Inland sediment movements by natural processes: Environmental Quality Lab Report No. 17-B, California Institute of Technology, Pasadena, 81p.

GRAIN SIZE DISTRIBUTIONS FOR STATION 1C

| MIDPOINT PHI--> | 0.50 | 1.50 | 2.50 | 3.50 | 4.50 | 5.50 | 6.50 | 7.50 | 8.50 | 9.50 | 10.50 |
|--------------------|------|------|------|-------|-------|-------|------|------|------|------|-------|
| 0-2 | 0.00 | 0.00 | 0.95 | 20.93 | 42.82 | 9.89 | 7.58 | 5.28 | 3.86 | 4.40 | 4.29 |
| 2-4 | 0.00 | 0.78 | 0.78 | 20.39 | 49.67 | 14.19 | 5.38 | 3.68 | 1.93 | 1.21 | 1.98 |
| 4-6 | 0.00 | 0.00 | 1.05 | 18.92 | 43.17 | 19.45 | 7.07 | 4.51 | 2.03 | 1.24 | 2.55 |
| 6-8 | 0.00 | 0.00 | 0.90 | 20.61 | 45.22 | 9.21 | 7.16 | 4.86 | 3.91 | 4.26 | 3.87 |
| 8-10 | 0.00 | 1.08 | 1.08 | 19.50 | 52.51 | 12.89 | 5.13 | 3.52 | 1.65 | 0.98 | 1.64 |

DOWNCORE SIZE DISTRIBUTIONS FOR STATION 3C

| midpoint phi--> | 0.50 | 1.50 | 2.50 | 3.50 | 4.50 | 5.50 | 6.50 | 7.50 | 8.50 | 9.50 | 10.50 |
|--------------------|------|------|------|-------|-------|-------|-------|-------|-------|------|-------|
| 0-2 cm | 0.00 | 0.00 | 4.00 | 18.02 | 26.13 | 10.36 | 10.07 | 9.88 | 5.61 | 6.76 | 9.17 |
| 2-4 | 0.00 | 0.00 | 5.34 | 26.68 | 35.42 | 7.76 | 6.72 | 5.22 | 3.52 | 3.00 | 6.34 |
| 4-6 | 0.00 | 0.00 | 4.51 | 22.56 | 28.99 | 11.05 | 7.33 | 7.49 | 6.91 | 3.56 | 7.61 |
| 6-8 | 0.00 | 0.00 | 5.75 | 23.00 | 32.97 | 13.17 | 9.29 | 6.38 | 4.02 | 2.91 | 2.52 |
| 8-10 | 0.00 | 0.00 | 4.01 | 17.36 | 29.19 | 9.54 | 11.44 | 7.09 | 8.31 | 3.67 | 9.38 |
| 10-12 | 0.00 | 1.01 | 8.12 | 8.12 | 28.14 | 21.77 | 14.54 | 7.92 | 5.76 | 5.68 | 6.05 |
| 12-14 | 0.00 | 0.00 | 1.45 | 5.06 | 24.29 | 14.20 | 13.15 | 13.75 | 11.57 | 5.41 | 11.14 |
| 14-16 | 0.00 | 0.00 | 0.89 | 5.34 | 29.16 | 21.77 | 12.81 | 8.44 | 5.83 | 6.15 | 9.61 |
| 16-18 | 0.00 | 0.00 | 0.99 | 5.94 | 19.20 | 14.04 | 13.88 | 13.33 | 18.85 | 1.66 | 12.09 |
| 18-20 | 0.00 | 0.00 | 1.15 | 5.73 | 26.37 | 21.41 | 14.62 | 8.51 | 5.33 | 6.88 | 10.00 |
| 20-22 | 0.00 | 0.00 | 2.79 | 15.32 | 23.74 | 11.34 | 8.12 | 11.73 | 9.09 | 7.15 | 10.72 |
| 22-24 | 0.00 | 0.00 | 2.26 | 12.46 | 28.77 | 17.94 | 12.20 | 7.19 | 5.09 | 5.01 | 9.07 |
| 24-26 | 0.00 | 4.67 | 2.34 | 25.70 | 26.75 | 8.27 | 6.53 | 6.31 | 5.51 | 4.13 | 9.79 |
| 26-28 | 0.00 | 2.98 | 2.98 | 35.72 | 35.91 | 5.75 | 4.60 | 2.71 | 2.37 | 2.19 | 4.80 |
| 28-30 | 0.00 | 0.00 | 3.48 | 34.83 | 35.45 | 7.90 | 4.17 | 2.93 | 3.44 | 1.45 | 6.35 |
| 30-32 | 0.00 | 1.59 | 4.78 | 22.29 | 32.60 | 11.13 | 9.27 | 5.48 | 4.86 | 4.77 | 3.24 |
| 32-34 | 0.00 | 1.60 | 4.80 | 27.18 | 41.29 | 8.36 | 5.02 | 2.83 | 2.36 | 3.57 | 2.98 |
| 34-36 | 0.00 | 0.00 | 8.21 | 24.62 | 40.43 | 7.98 | 4.86 | 2.34 | 2.34 | 2.00 | 6.72 |
| 36-38 | 1.39 | 1.39 | 5.57 | 25.09 | 35.46 | 9.35 | 7.29 | 3.81 | 3.48 | 3.95 | 3.21 |
| 38-40 | 0.00 | 3.22 | 6.45 | 29.02 | 38.57 | 7.82 | 4.21 | 2.68 | 1.57 | 3.06 | 3.41 |

GRAIN SIZE DISTRIBUTION STATION OC

| MIDPOINT PHI --> | 0.50 | 1.50 | 2.50 | 3.50 | 4.50 | 5.50 | 6.50 | 7.50 | 8.50 | 9.50 | 10.50 |
|---------------------|------|------|------|-------|-------|-------|------|------|------|------|-------|
| 0-2 | 0.00 | 0.00 | 0.00 | 13.69 | 59.01 | 9.87 | 3.34 | 3.34 | 4.51 | 1.17 | 5.06 |
| 4-6 | 0.00 | 0.00 | 1.73 | 10.40 | 58.24 | 10.11 | 4.19 | 4.78 | 3.71 | 2.21 | 4.62 |
| 8-10 | 0.00 | 0.00 | 0.00 | 14.27 | 55.81 | 11.46 | 4.54 | 3.36 | 4.13 | 1.89 | 4.55 |
| 12-14 | 0.00 | 0.00 | 0.00 | 16.81 | 56.94 | 9.58 | 3.72 | 3.72 | 3.54 | 1.16 | 4.53 |

GRAIN SIZE DISTRIBUTION STATION 6C

| MIDPOINT PHI--> | 0.50 | 1.50 | 2.50 | 3.50 | 4.50 | 5.50 | 6.50 | 7.50 | 8.50 | 9.50 | 10.50 |
|--------------------|------|------|------|-------|-------|-------|-------|------|--------|-------|-------|
| 0-2 | 0.00 | 0.00 | 0.00 | 6.06 | 49.32 | 17.95 | 10.99 | 4.82 | -13.01 | 19.86 | 4.02 |
| 2-4 | 0.00 | 0.00 | 0.00 | 6.45 | 54.70 | 18.40 | 7.72 | 4.85 | 2.69 | 2.06 | 3.12 |
| 4-6 | 0.00 | 0.00 | 0.00 | 6.54 | 58.84 | 16.67 | 6.54 | 3.87 | 2.67 | 1.93 | 2.93 |
| 6-8 | 0.00 | 0.00 | 0.00 | 4.91 | 51.59 | 20.82 | 8.25 | 5.39 | 3.10 | 2.45 | 3.49 |
| 8-10 | 0.00 | 0.00 | 0.00 | 3.67 | 49.95 | 20.89 | 8.55 | 6.09 | 3.24 | 3.47 | 4.15 |
| 10-12 | 0.00 | 0.00 | 0.00 | 2.80 | 40.46 | 25.27 | 10.34 | 6.93 | 4.23 | 4.35 | 5.62 |
| 12-14 | 0.00 | 0.00 | 0.00 | 2.17 | 42.33 | 22.43 | 12.77 | 4.66 | 3.89 | 5.00 | 6.75 |
| 14-16 | 0.00 | 0.00 | 0.00 | 2.15 | 39.10 | 23.73 | 11.68 | 6.39 | 4.18 | 5.78 | 6.98 |
| 16-18 | 0.00 | 0.00 | 0.00 | 2.59 | 42.13 | 22.23 | 11.40 | 6.05 | 4.22 | 4.93 | 6.45 |
| 18-20 | 0.00 | 0.00 | 0.00 | 2.23 | 44.05 | 20.24 | 11.13 | 6.43 | 4.02 | 5.23 | 6.68 |
| 20-22 | 0.00 | 0.00 | 0.00 | 1.91 | 35.08 | 22.43 | 12.21 | 7.70 | 5.04 | 6.77 | 8.87 |
| 22-24 | 0.00 | 0.00 | 0.00 | 1.50 | 34.72 | 22.59 | 12.86 | 8.77 | 5.29 | 5.89 | 8.39 |
| 24-26 | 0.00 | 0.00 | 0.00 | 1.66 | 36.15 | 21.04 | 12.68 | 7.45 | 5.36 | 6.40 | 9.25 |
| 26-28 | 0.00 | 0.00 | 0.00 | 1.69 | 35.00 | 22.13 | 12.36 | 6.83 | 5.41 | 6.83 | 9.75 |
| 28-30 | 0.00 | 0.00 | 0.00 | 2.47 | 36.04 | 24.06 | 11.71 | 7.08 | 4.89 | 5.79 | 7.95 |
| 30-32 | 0.00 | 0.00 | 0.00 | 3.58 | 35.54 | 25.68 | 11.79 | 6.42 | 4.63 | 5.37 | 6.99 |
| 32-34 | 0.00 | 0.00 | 0.00 | 3.43 | 39.71 | 25.95 | 10.05 | 5.85 | 2.44 | 6.63 | 5.93 |
| 34-36 | 0.00 | 0.00 | 0.00 | 5.20 | 40.80 | 22.78 | 9.92 | 5.78 | 3.74 | 5.21 | 6.57 |
| 36-38 | 0.00 | 0.00 | 0.00 | 6.19 | 39.57 | 24.14 | 10.72 | 6.06 | 3.76 | 4.75 | 4.81 |
| 38-40 | 0.00 | 0.00 | 0.00 | 8.18 | 49.98 | 18.61 | 8.04 | 5.07 | 3.33 | 3.26 | 3.53 |
| 40-42 | 0.00 | 0.00 | 0.00 | 11.75 | 58.34 | 16.63 | 4.87 | 3.30 | 1.95 | 1.40 | 1.77 |
| 42-44 | 0.00 | 0.00 | 0.00 | 11.76 | 62.90 | 14.86 | 5.16 | 2.86 | 0.87 | 0.56 | 1.03 |
| 44-46 | 0.00 | 0.00 | 0.00 | 11.36 | 52.69 | 22.43 | 8.13 | 3.11 | 0.82 | 0.43 | 0.83 |
| 46-48 | 0.00 | 0.00 | 0.58 | 12.67 | 59.50 | 15.42 | 6.98 | 2.76 | 0.80 | 0.46 | 0.83 |
| 48-50 | 0.00 | 0.00 | 0.00 | 11.81 | 60.22 | 15.79 | 6.55 | 3.28 | 0.85 | 0.48 | 1.02 |

GRAIN SIZE DISTRIBUTIONS STATION 8C

| MIDPOINT PHI--> | -1.50 | -0.50 | 0.50 | 1.50 | 2.50 | 3.50 | 4.50 | 5.50 | 6.50 | 7.50 | 8.50 | 9.50 | 10.50 |
|--------------------|-------|-------|------|-------|-------|------|-------|-------|-------|-------|------|------|-------|
| 0-2 | 0.31 | 0.54 | 0.75 | 1.55 | 1.82 | 6.73 | 44.86 | 13.12 | 9.15 | 6.28 | 2.68 | 5.36 | 6.85 |
| 2-4 | 0.41 | 0.26 | 0.71 | 2.80 | 3.91 | 6.63 | 39.11 | 15.05 | 10.75 | 7.01 | 3.96 | 3.85 | 5.57 |
| 4-6 | 0.19 | 0.63 | 0.55 | 2.66 | 3.36 | 6.49 | 34.39 | 17.52 | 11.15 | 7.38 | 4.78 | 5.07 | 5.82 |
| 6-8 | 0.31 | 0.63 | 1.52 | 5.38 | 4.91 | 4.36 | 33.13 | 16.27 | 10.50 | 6.81 | 4.6 | 5.66 | 5.91 |
| 8-10 | 0.47 | 1.20 | 1.40 | 3.75 | 3.21 | 3.45 | 32.45 | 18.48 | 11.90 | 7.00 | 4.6 | 5.88 | 6.19 |
| 10-12 | 2.71 | 2.45 | 2.65 | 4.55 | 4.08 | 1.68 | 16.30 | 21.20 | 13.81 | 8.36 | 6.42 | 6.07 | 8.85 |
| 12-14 | 1.15 | 1.97 | 2.33 | 4.31 | 4.63 | 2.23 | 20.32 | 20.36 | 13.70 | 7.83 | 6.22 | 6.54 | 7.90 |
| 14-16 | 1.65 | 3.01 | 3.60 | 7.59 | 5.28 | 1.93 | 15.38 | 20.07 | 12.87 | 8.29 | 5.89 | 7.49 | 8.15 |
| 16-18 | 0.00 | 0.09 | 0.24 | 0.87 | 1.29 | 2.01 | 26.00 | 23.89 | 15.14 | 8.90 | 6.97 | 8.50 | 8.37 |
| 18-20 | 0.17 | 0.96 | 1.01 | 1.28 | 1.07 | 0.30 | 18.48 | 26.36 | 15.81 | 10.71 | 6.30 | 7.26 | 7.94 |
| 20-22 | 2.86 | 1.54 | 1.85 | 3.05 | 2.31 | 1.23 | 19.32 | 22.28 | 15.17 | 7.22 | 4.93 | 4.75 | 7.96 |
| 22-24 | 2.10 | 4.60 | 5.67 | 15.66 | 7.64 | 1.37 | 9.91 | 17.61 | 10.57 | 8.31 | 6.00 | 6.92 | 10.20 |
| 24-26 | 1.19 | 2.84 | 2.72 | 7.24 | 4.96 | 1.70 | 9.16 | 23.07 | 15.69 | 10.12 | 7.40 | 7.90 | 11.65 |
| 26-28 | 1.07 | 1.26 | 1.78 | 3.51 | 3.32 | 1.70 | 15.50 | 20.48 | 14.31 | 7.44 | 5.67 | 7.61 | 8.54 |
| 28-30 | 0.83 | 1.85 | 2.06 | 2.70 | 1.76 | 1.30 | 14.32 | 22.75 | 15.03 | 6.06 | 1.04 | 7.10 | 4.02 |
| 30-32 | 0.53 | 1.65 | 1.94 | 5.60 | 4.74 | 1.86 | 17.78 | 21.60 | 15.05 | 7.79 | 5.19 | 5.88 | 6.86 |
| 32-34 | 1.57 | 3.78 | 3.56 | 7.20 | 7.83 | 2.55 | 23.74 | 21.49 | 12.03 | 8.78 | 6.10 | 6.68 | 7.49 |
| 34-36 | 2.88 | 3.31 | 3.37 | 6.99 | 5.10 | 1.55 | 19.91 | 19.13 | 15.07 | 9.28 | 6.13 | 7.52 | 7.52 |
| 36-38 | 1.12 | 1.42 | 1.98 | 4.33 | 3.19 | 1.67 | 17.00 | 25.18 | 14.25 | 6.03 | 6.02 | 4.75 | 5.76 |
| 38-40 | 2.04 | 2.82 | 2.34 | 6.05 | 4.56 | 1.97 | 16.20 | 18.80 | 11.86 | 8.03 | 4.57 | 5.12 | 4.57 |
| 40-42 | 2.34 | 3.27 | 3.25 | 6.71 | 8.22 | 1.68 | 16.97 | 15.98 | 9.80 | 6.03 | 4.32 | 4.57 | 4.57 |
| 42-44 | 3.11 | 4.87 | 5.04 | 12.76 | 6.69 | 2.42 | 16.92 | 16.45 | 10.80 | 5.82 | 4.75 | 4.75 | 5.93 |
| 44-46 | 1.83 | 3.72 | 4.35 | 17.01 | 6.18 | 1.39 | 18.67 | 21.60 | 12.82 | 4.90 | 5.47 | 4.75 | 4.42 |
| 46-48 | 1.20 | 2.41 | 2.32 | 12.36 | 6.18 | 1.39 | 18.67 | 21.60 | 12.82 | 4.90 | 5.47 | 4.75 | 4.42 |
| 48-50 | 2.52 | 2.47 | 2.21 | 13.57 | 15.32 | 2.81 | 16.63 | 16.32 | 9.56 | 6.12 | 3.76 | 4.30 | 4.30 |

GRAIN SIZE DISTRIBUTIONS STATION 9C

| MIDPOINT PHI--> | 0.50 | 1.50 | 2.50 | 3.50 | 4.50 | 5.50 | 6.50 | 7.50 | 8.50 | 9.50 | 10.50 |
|--------------------|------|------|------|-------|-------|-------|-------|-------|------|------|-------|
| 0-2 | 0.00 | 0.00 | 0.00 | 19.76 | 43.08 | 9.40 | 6.83 | 5.50 | 4.84 | 0.00 | 10.59 |
| 2-4 | 0.00 | 0.00 | 1.04 | 14.58 | 50.32 | 19.23 | 5.37 | 4.04 | 2.05 | 1.21 | 2.16 |
| 4-6 | 0.00 | 0.00 | 1.43 | 11.43 | 30.71 | 11.11 | 10.01 | 10.28 | 8.08 | 6.65 | 10.30 |
| 6-8 | 0.00 | 0.00 | 0.94 | 8.46 | 37.98 | 29.55 | 8.02 | 5.76 | 3.49 | 2.52 | 3.29 |
| 8-10 | 0.00 | 0.00 | 0.00 | 11.04 | 27.62 | 13.68 | 11.69 | 10.58 | 7.99 | 5.70 | 11.71 |
| R-10 | 0.00 | 0.00 | 0.00 | 27.65 | 41.61 | 9.76 | 5.81 | 3.47 | 3.31 | 2.62 | 5.78 |

GRAIN SIZE DISTRIBUTIONS STATION 5D

| MIDPOINT PHI--> | -0.50 | 0.50 | 1.50 | 2.50 | 3.50 | 4.50 | 5.50 | 6.50 | 7.50 | 8.50 | 9.50 | 10.50 |
|--------------------|-------|-------|-------|-------|------|------|------|------|------|------|------|-------|
| 0-2 | 0.00 | 26.12 | 37.74 | 5.81 | 2.90 | 9.72 | 4.32 | 3.71 | 1.74 | 4.06 | 1.61 | 2.27 |
| 2-4 | 2.70 | 32.73 | 29.10 | 5.46 | 3.64 | 8.10 | 6.93 | 5.59 | 2.96 | 1.73 | 0.72 | 1.24 |
| 4-6 | 0.00 | 36.80 | 36.80 | 3.35 | 3.35 | 5.26 | 3.85 | 3.40 | 0.00 | 4.69 | 0.95 | 1.56 |
| 6-8 | 4.56 | 33.39 | 27.32 | 6.07 | 3.04 | 6.80 | 6.90 | 5.76 | 3.13 | 2.03 | 1.28 | 1.26 |
| 8-10 | 0.00 | 28.24 | 26.48 | 3.53 | 1.77 | 9.12 | 6.97 | 6.69 | 2.60 | 7.79 | 2.57 | 4.26 |
| 10-12 | 0.00 | 33.22 | 28.24 | 3.32 | 4.98 | 7.92 | 5.06 | 5.98 | 3.63 | 2.80 | 2.90 | 1.95 |
| 12-14 | 0.00 | 26.61 | 31.05 | 8.87 | 4.44 | 7.68 | 5.52 | 4.79 | 3.53 | 3.37 | 1.59 | 2.55 |
| 14-16 | 0.00 | 29.36 | 34.25 | 9.79 | 4.89 | 5.64 | 5.20 | 4.72 | 2.60 | 1.47 | 1.27 | 0.83 |
| 16-18 | 0.00 | 31.82 | 31.82 | 3.54 | 7.07 | 7.17 | 4.52 | 4.44 | 2.84 | 3.00 | 1.40 | 2.37 |
| 18-20 | 0.00 | 38.06 | 33.83 | 4.23 | 4.23 | 5.32 | 5.10 | 4.24 | 2.07 | 1.62 | 0.45 | 0.84 |
| 20-22 | 0.00 | 27.19 | 32.63 | 16.31 | 5.44 | 5.62 | 3.41 | 3.24 | 1.86 | 1.93 | 0.95 | 1.42 |
| 22-24 | 6.13 | 44.37 | 27.30 | 6.83 | 3.41 | 3.71 | 3.54 | 2.98 | 1.59 | 0.95 | 0.84 | 1.07 |
| 24-26 | 4.61 | 37.50 | 34.61 | 8.65 | 2.88 | 3.10 | 3.04 | 2.94 | 1.82 | 0.90 | 0.61 | 1.06 |
| 26-28 | 0.00 | 31.52 | 34.68 | 9.46 | 3.15 | 4.71 | 5.51 | 4.49 | 2.50 | 1.54 | 1.20 | 1.24 |
| 28-30 | 2.19 | 43.81 | 30.67 | 4.38 | 4.38 | 3.70 | 3.34 | 3.03 | 1.54 | 0.31 | 1.67 | 0.99 |

GRAIN SIZE DISTRIBUTIONS STATION 8D

| MIDPOINT PHI --> | -0.50 | 0.50 | 1.50 | 2.50 | 3.50 | 4.50 | 5.50 | 6.50 | 7.50 | 8.50 | 9.50 | 10.50 |
|---------------------|-------|------|------|-------|-------|-------|-------|-------|------|------|------|-------|
| 0-2 | 0.00 | 0.00 | 0.00 | 9.88 | 42.83 | 24.69 | 6.05 | 4.21 | 3.79 | 2.63 | 2.26 | 3.65 |
| 2-4 | 0.00 | 0.00 | 2.68 | 5.35 | 40.13 | 30.42 | 7.17 | 4.91 | 3.20 | 2.22 | 2.09 | 1.85 |
| 4-6 | 0.00 | 0.00 | 0.00 | 7.00 | 42.02 | 27.57 | 5.50 | 4.71 | 2.75 | 2.42 | 1.21 | 6.82 |
| 6-8 | 0.00 | 0.00 | 2.17 | 10.83 | 34.65 | 25.52 | 9.39 | 6.19 | 3.66 | 2.63 | 2.53 | 2.44 |
| 8-10 | 0.00 | 0.00 | 0.00 | 9.88 | 39.53 | 26.66 | 6.33 | 4.41 | 3.98 | 2.40 | 2.35 | 4.46 |
| 10-12 | 0.00 | 0.00 | 1.86 | 12.99 | 37.12 | 24.79 | 7.53 | 4.89 | 2.08 | 2.08 | 2.31 | 2.49 |
| 12-14 | 0.00 | 0.00 | 3.49 | 13.95 | 41.84 | 19.35 | 5.04 | 4.92 | 2.64 | 2.11 | 2.44 | 4.23 |
| 14-16 | 0.00 | 0.00 | 3.51 | 10.53 | 33.34 | 26.88 | 7.66 | 6.06 | 3.48 | 2.57 | 2.84 | 3.12 |
| 16-18 | 0.00 | 0.00 | 3.79 | 6.98 | 30.29 | 22.15 | 8.27 | 6.02 | 5.44 | 4.74 | 3.07 | 4.88 |
| 18-20 | 0.81 | 3.41 | 5.50 | 6.98 | 24.43 | 24.54 | 11.05 | 7.15 | 4.05 | 3.26 | 3.16 | 4.91 |
| 20-22 | 0.00 | 0.00 | 2.60 | 5.20 | 26.01 | 23.29 | 9.56 | 8.93 | 7.36 | 5.78 | 4.40 | 6.80 |
| 22-24 | 1.17 | 3.16 | 3.83 | 4.11 | 9.86 | 17.82 | 15.76 | 10.30 | 6.46 | 4.34 | 4.55 | 6.80 |
| 24-26 | 2.76 | 5.29 | 2.75 | 2.37 | 8.93 | 15.66 | 13.10 | 10.74 | 9.64 | 8.23 | 5.62 | 8.36 |
| 26-28 | 3.40 | 8.06 | 5.31 | 4.40 | 12.06 | 20.15 | 8.94 | 8.94 | 6.19 | 4.69 | 4.16 | 6.84 |
| 28-30 | 4.94 | 3.62 | 5.03 | 5.67 | 20.27 | 21.58 | 9.13 | 7.06 | 6.50 | 5.19 | 3.63 | 6.27 |

GRAIN SIZE DISTRIBUTION FOR STATION 1A

| MIDPOINT PHI--> | 0.50 | 1.50 | 2.50 | 3.50 | 4.50 | 5.50 | 6.50 | 7.50 | 8.50 | 9.50 | 10.50 |
|--------------------|------|------|------|-------|-------|-------|-------|-------|------|------|-------|
| 0-2 | 0.00 | 1.27 | 1.27 | 16.49 | 57.67 | 7.52 | 4.71 | 3.24 | 2.62 | 2.52 | 2.68 |
| 4-6 | 0.00 | 0.00 | 1.01 | 13.18 | 47.85 | 16.67 | 8.82 | 6.10 | 2.79 | 1.69 | 1.91 |
| 10-12 | 0.00 | 0.00 | 0.00 | 5.39 | 31.63 | 19.19 | 28.23 | 11.06 | 0.85 | 1.89 | 1.78 |
| 16-18 | 0.00 | 0.00 | 0.00 | 2.63 | 22.33 | 18.19 | 35.67 | 14.70 | 3.32 | 0.81 | 2.37 |

GRAIN SIZE DISTRIBUTIONS FOR STATION 3A

| MIDPOINT PHI--> | 0.50 | 1.50 | 2.50 | 3.50 | 4.50 | 5.50 | 6.50 | 7.50 | 8.50 | 9.50 | 10.50 |
|--------------------|------|------|------|-------|-------|-------|-------|------|------|------|-------|
| 0-2 | 0.00 | 0.00 | 0.00 | 3.74 | 38.77 | 20.77 | 12.59 | 7.64 | 4.84 | 5.92 | 5.72 |
| 4-6 | 0.00 | 0.00 | 0.00 | 9.26 | 56.92 | 14.81 | 6.61 | 5.08 | 3.00 | 2.02 | 2.29 |
| 8-10 | 0.00 | 0.00 | 0.00 | 7.91 | 41.42 | 22.03 | 11.96 | 8.02 | 3.94 | 2.20 | 2.53 |
| 14-16 | 0.00 | 0.00 | 0.00 | 11.88 | 55.64 | 13.34 | 8.10 | 5.18 | 2.76 | 1.27 | 1.84 |
| 20-22 | 0.00 | 0.00 | 0.00 | 13.03 | 64.05 | 8.48 | 5.76 | 3.75 | 2.12 | 1.20 | 1.60 |

GRAIN SIZE DISTRIBUTIONS STATION 6A

| MIDPOINT PHI--> | 0.50 | 1.50 | 2.50 | 3.50 | 4.50 | 5.50 | 6.50 | 7.50 | 8.50 | 9.50 | 10.50 |
|--------------------|------|------|------|-------|-------|-------|-------|-------|------|------|-------|
| 0-2 | 0.00 | 0.00 | 0.88 | 9.65 | 39.22 | 19.29 | 11.72 | 6.94 | 3.43 | 5.02 | 3.86 |
| 2-4 | 0.00 | 0.00 | 0.00 | 13.44 | 45.38 | 20.10 | 8.67 | 5.63 | 3.10 | 1.58 | 2.11 |
| 4-6 | 0.00 | 0.00 | 0.00 | 9.33 | 44.91 | 21.60 | 10.44 | 6.27 | 3.46 | 1.63 | 2.36 |
| 6-8 | 0.00 | 0.00 | 0.00 | 7.92 | 39.95 | 23.37 | 12.95 | 7.08 | 4.06 | 2.14 | 2.55 |
| 8-10 | 0.00 | 0.00 | 0.00 | 7.35 | 36.85 | 25.92 | 13.30 | 8.27 | 3.72 | 2.07 | 2.51 |
| 10-12 | 0.00 | 0.00 | 0.00 | 7.61 | 36.78 | 21.65 | 15.82 | 9.14 | 4.26 | 2.13 | 2.60 |
| 12-14 | 0.00 | 0.00 | 0.00 | 11.11 | 50.74 | 12.34 | 10.86 | 6.24 | 3.85 | 2.24 | 2.62 |
| 14-16 | 0.00 | 0.00 | 0.00 | 11.45 | 51.97 | 14.19 | 11.55 | 6.73 | 1.74 | 0.90 | 1.47 |
| 16-18 | 0.00 | 0.00 | 0.00 | 8.19 | 42.58 | 15.56 | 19.55 | 9.45 | 1.99 | 0.90 | 1.76 |
| 18-20 | 0.00 | 0.00 | 0.00 | 8.34 | 42.44 | 13.70 | 18.71 | 11.19 | 2.42 | 1.00 | 2.20 |
| 20-22 | 0.00 | 0.00 | 0.00 | 7.13 | 47.32 | 13.38 | 17.75 | 9.73 | 2.00 | 0.83 | 1.85 |
| 22-24 | 0.00 | 0.00 | 0.00 | 6.38 | 51.86 | 13.37 | 14.99 | 8.58 | 2.04 | 0.90 | 1.88 |
| 24-26 | 0.00 | 0.00 | 0.00 | 7.33 | 48.97 | 13.96 | 14.96 | 9.08 | 2.60 | 1.07 | 2.03 |
| 26-28 | 0.00 | 0.00 | 0.00 | 6.28 | 55.07 | 12.62 | 12.62 | 7.89 | 2.46 | 1.10 | 1.97 |